BLAST RESISTANT DESIGN OF RC FRAMES

A DISSERTATION

Submitted in partial fulfilment of the

requirements for the award of the degree

of

MASTER OF TECHNOLOGY

in

CIVIL ENGINEERING

(With Specialization in Structural Engineering)

By

ROHAN AGARWAL

(17523020)

DEPARTMENT OF CIVIL ENGINEERING

INDIAN INSTITUTE OF TECHNOLOGY ROORKEE

ROORKEE – 247 667 (INDIA)

MAY, 2019

CANDIDATE'S DECLARATION

I hereby declare that work presented in this dissertation has been carried out by me in the Department of Civil Engineering at Indian Institute of Technology Roorkee under the supervision of **Dr. Pradeep Bhargava**, Professor, Department of Civil Engineering, IIT Roorkee. The matter embodied in this dissertation has not been submitted for the award of any other degree.

Date: 20th May, 2019 (Rohan Agarwal)

Place: Roorkee 17523020

CERTIFICATE

This is to certify that the report entitled, **Blast Resistant Design of RC Frames** submitted by **Rohan Agarwal**, embodies the work done by him under my supervision.

Date: 20th May, 2019 (Dr. Pradeep Bhargava)

Professor,

Department of Civil Engineering,

Indian Institute of Technology Roorkee

ACKNOWLEDGEMENT

Foremost, I would like to express my profound and sincere gratitude towards my supervisor, Dr. Pradeep Bhargava, Professor, Department of Civil Engineering, Indian Institute of Technology Roorkee for his inspiring guidance, patience, motivation, enthusiasm and immense knowledge. His guidance and constant encouragement helped me throughout the course of this work. I could not have imagined having a better advisor and mentor, whose moral and material support was priceless. It was an opportunity of a life time to be associated with him.

I would also like to express my special thanks and appreciation to Mr. M. Ravi Kumar for his help, motivation and inspiration which provided me a high mental

Date: 20th May 2019 Rohan Agarwal

Place: Roorkee (17523020)

ABSTRACT

Proper control levels of lateral drifts anticipated for reinforced concrete (RC) frame structures within the predefined performance level becomes crucial when the frame structure is subjected to distant intense surface explosions. For this purpose, a design method is presented based on the transformation of a blast loading into an equivalent static force (ESF). The ESF is calculated in such a manner that the same maximum inter-storey drift ratio (MIDR) under the blast loading will be reproduced. The work focuses on the computational model of ESF for a single-degree-of-freedom (SDOF) system and the design method based on ESF with the requirement for controlling its maximum displacement response to achieve the specified target displacement. The model for the calculation of an equivalent static force (ESF) for SDOF systems is extended into the design for a reinforced concrete (RC) frame structure under distant blast conditions. The use of the method is demonstrated with two six-storey RC frame structures and one nine-storey RC frame. The results indicate that the maximum inter-storey drift ratios (MIDR) of the three designed frame structures in comparison to their respective targets are conservative to some extent.

Keywords: Maximum inter-storey drift ratio; Equivalent static force; Reinforced concrete frame structure; Blast loading; Blast Resistant Design

Contents

List of Figures		
Figure no.	Description	Page no.
2.1	Bomb attack on Murrah Federal Building in Oklahoma city, 1995, (a, b) before the attack (c, d) after the attack	3
2.2	Unconfined explosions	5
2.3	Internal blast categories	6
2.4	Ideal free air blast wave Pressure-Time history	6
2.5	Simplified blast wave overpressure profile	9
2.6	Strain rates for different loading conditions	10
3.1	Two classes of blast wave-surface interaction	12
3.2	Details of the target six-storey frame structure	14
3.3	Positive phase shock wave parameters for a hemispherical TNT explosion on the surface at sea level	15
3.4	Blast dynamic pressure causing push on front face of target followed by suction force on top and rear as blast waves pass over and round the target	16
3.5	Blast loading on various sides of structure	18
3.6	Stress-strain plot for Concrete M40	18
3.7	Plastic Hinge Model per FEMA-356 (IO = immediate occupancy, LS = life safety, CP = collapse prevention)	19
4.1 (a)	Dynamic response process of the original SDOF system under the blast force	22
4.1	Process for the construction of ESF for a SDOF system	23
4.2	Three different response states for a SDOF system at the time t_d and t_m	26
4.3	Distribution of the ESF factor for the SDOF system	30
5.1	Process for ESF construction for an RC frame structure	34
6.1	RC frame having a uniform lateral blast pressure and a DL acting vertically = 30 KN/m	36
6.2	Flowchart of blast resistant design of a multi-storey reinforced concrete frame structure with ESF (e_1 is an arbitrarily small value)	37
6.3	Sectional Detail	38

List of Tables

CHAPTER 1

INTRODUCTION

1.1 General

There has been in growing concern among citizens in the past few decades regarding the safety and durability of important civil structures due to the rise in the number of terrorist attacks. Terrorists use fear and confusion to create mayhem in the society and in the political circles by using very less fire power than conventional military. Therefore, the use of explosives to target civilian buildings and other structures is becoming a growing problem in modern society. Explosives have become smaller in size and more powerful these days leading to its increased mobility and larger range effects.**[9]** Casualties from such explosions not only result in immediate loss of life due to release of huge amount of energy but also compromises the structure strength and integrity leading to extensive life loss. After the 9/11 bombing of World Trade Centre in USA, areas of high people concentration such as government buildings, metro and train stations, and stadiums have been given attention to maximize its potential to provide protection against explosive effects. Thus, the effect of blast loads on buildings has become a serious matter that should be taken into consideration in the design process.**[1]**

Blast analysis of structures is complex as it involves various parameters related to non-linearity and dynamic strength factor under rapid strain rate.**[12]** Since, most of the civilian reinforced concrete frame structures have multi-storey levels, the identification of the dynamic behaviour and damage distribution of multi-storey reinforced concrete frame structures under the intense surface explosion conditions become increasingly important.

To mitigate the effects of blast impact on a building, retrofitting the structural components such as load bearing columns and key elements where blast pressure is directly applied can be carried out. Buildings may undergo progressive collapse due to transfer of load from members that have undergone catastrophic failure.

1.2 Research Objectives and Scopes

This thesis focuses on analyzing the dynamic responses for Multi-storey Reinforced Concrete frame structures under distant surface blast loading conditions. The method for blast resistant design is based on the transformation of the distant blast loading into the

equivalent static force (ESF). Since the case discussed is for distant blast, where the hemispherical surface blast wave produced may be reasonably simplified to a uniform lateral planar wave, the maximum inter-

Storey drift ratio (IDR) response parameter is taken as the global performance indicator. The ESF is calculated in such a way that the same MIDR effect will be produced as that under the distant blast condition. The following list outlines the scope of the work carried out in this thesis:

a) Calculation of blast pressure and loading parameters on a closed 6-storey reinforced concrete building using IS 4991-1968 and TM5-1300.

b) Procedure for development of ESF for a single degree of freedom system

c) Procedure for development of ESF for a multi degree of freedom system

d) A planar six-storey RC frame structure is subjected to explosions of 80 t TNT at 100m and 30 t TNT at 100m. The uniform lateral blast pressure is applied only on the front face of the building. The design objective is to ensure that the Maximum Inter-storey Drift Ratio (MIDR) of the designed structural system is within the expected performance level defined by the target MIDR.

e) A planar nine-storey RC frame subjected to 30t TNT explosion at 100m is now subjected to the blast pressure on the front face of the building and the MIDR is ensured within the target.

The superimposed Dead Load of 30 KN/m accompanies the blast load for all the above cases. The analysis is carried out in ETABS-2015 software package.

CHAPTER 2

LITERATURE REVIEW

2.1 Explosion

An explosion involves chemical reaction resulting in a sudden burst of energy on a large scale in a very small span of time. This sudden release of energy increases the surrounding temperature (about 3000^{o}C) and pressure (about 3x10^{7} Pa). This high pressure gas travels with high velocity to areas far from origin of the incident. **[16]**

Fig 2.1.: Bomb attack on Murrah Federal Building in Oklahoma city, 1995, (a, b) before the attack (c, d) after the attack **[9]**

2.2 TNT Equivalency

Explosive materials available could vary from homemade to military or commercially available types and these differ from one another by their explosion characteristics such as detonation rate, effectiveness, and amount of energy released. Therefore, TNT has been used as a datum explosive and is regarded as "Explosive Bench Mark"**[16]** to assess the detonation characteristics of each types of explosive material. The effects of various

explosive materials are expressed in terms of standard TNT equivalent mass using the equation below.

$$W_E = \frac{H_{exp}}{H_{TNT}} X\, W_{exp}$$

Here, W_E = effective charge weight (in TNT)

W_{exp} = weight of the explosive in question

H_{exp} = heat of detonation of explosive in question

H_{TNT} = heat of detonation of TNT

Some conversion factors for common explosive material are shown in Table 2.1.

Table 2-1: TNT equivalent of common explosives materials [17]

Explosive	TNT Equivalent
ANFO	0.82
Composition A-3	1.09
HMX	1.3
PETN	1.27
RDX	1.2
Tetryt1	1.07
TNETB	1.36
TNT	1
TRITONAL	1.07

2.3 Blast Loading Types

Explosions are classified into two major categories **[16]**

- External explosions – occur in an open environment
- Internal explosions – occur inside a covered container or building

If the classification is made based on the characteristics of the approach blast waves towards a particular structure, it can be classified as below. **[17]**

- Unconfined
- Confined
- Explosive attached to a structure.

Unconfined explosions can be further classified into three kinds of bursts, namely free air burst, air burst and surface burst. If the explosion occurred in free air high above ground level, it is classified as a free-air burst explosion. If the explosion occurs in free air above ground level, but is accompanied by amplification of blast wave due to ground reflections,

it is called Air Burst. A surface burst occurs when the blast takes place close to or on the ground surface. Surface burst is usually accompanied by reflection from the ground surface resulting in reflected over-pressure. The above three types of Unconfined explosions are shown in Figure 2.2.

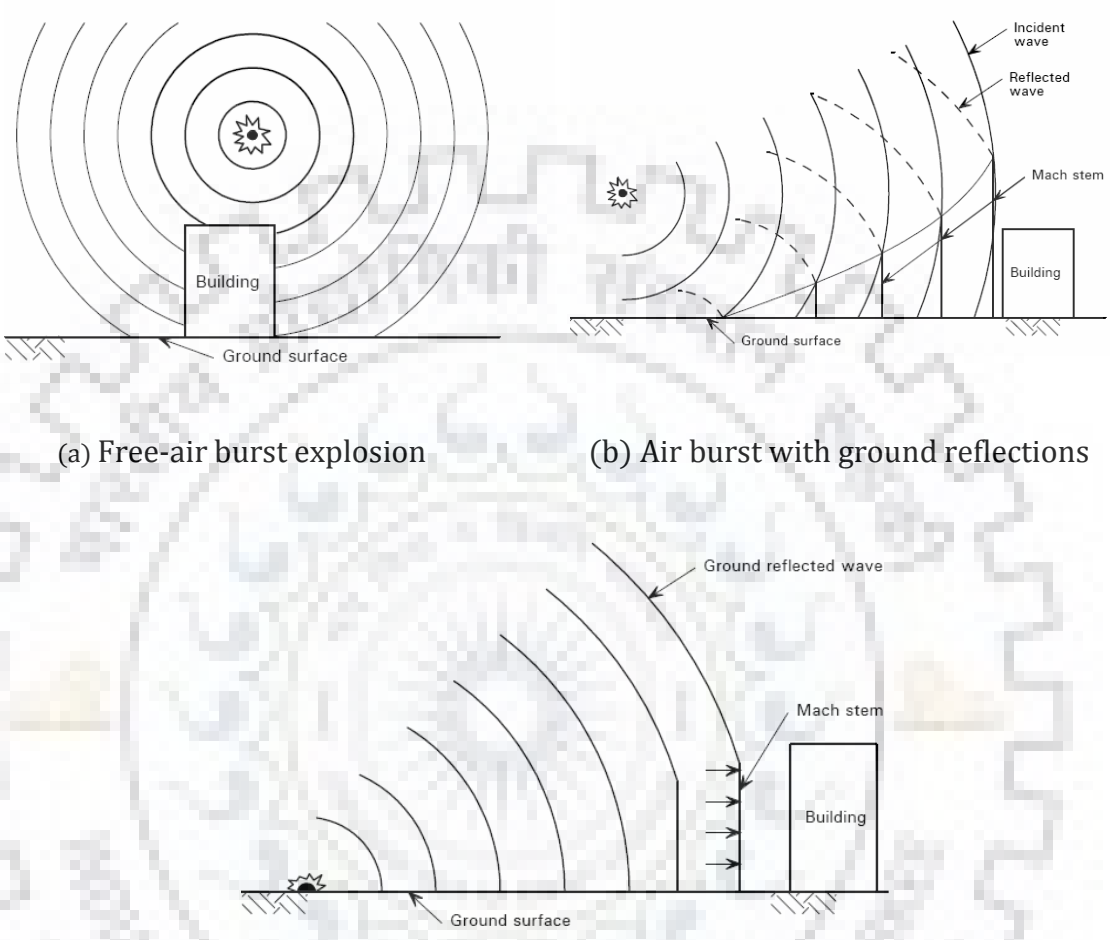

(a) Free-air burst explosion (b) Air burst with ground reflections

(c) Surface burst

Fig. 2.2.: Unconfined explosions [17]

When a detonation occurs within a structure, the explosion can be further categorized as

- Fully vented
- Partially vented
- Fully confined

A fully vented confined explosion is created within a structure, which has one or more opening surfaces to the atmosphere. If the vented surfaces are more limited than a fully confined case, it is said to be a partially vented confined explosion. If it happens in a fully covered volume, it becomes a fully confined explosion. Figure 2-3 illustrates each of these internal blasts. **[17]**

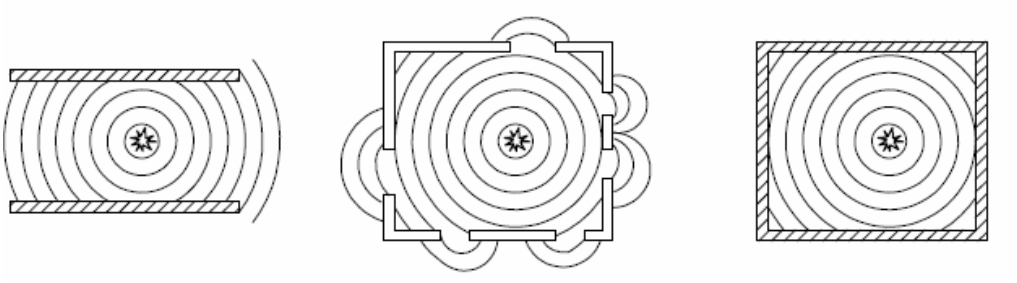

(a) Fully vented (b) Partially vented (c) Fully confined

Fig. 2.3.: Internal blast categories [17]

2.4. Blast Load Characteristics

Blast loads being dynamic in nature is characterized by its pressure intensity and duration **[11]**.

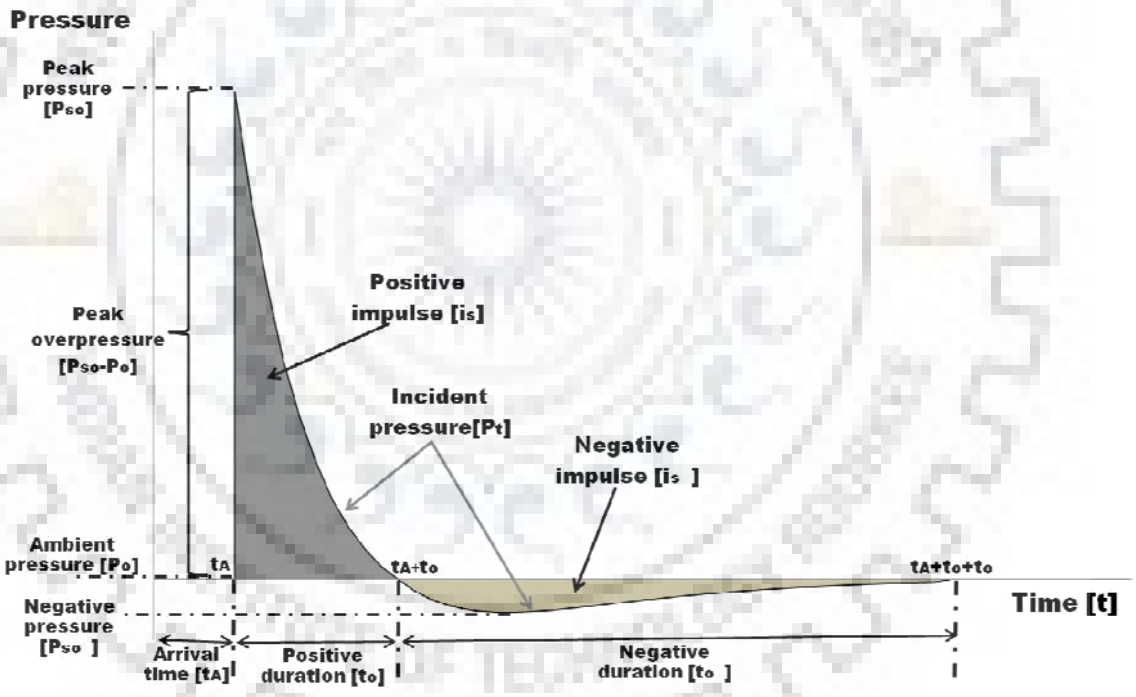

Fig. 2.4.: Ideal free air blast wave Pressure-Time history [10]

The parameters that describe blast loads are given by TM5-1300 1990, Yandzio et al. 1999:

- Arrival time, t_A: The time taken to reach the blast pressure at a particular point after the explosion occurred.
- Ambient pressure, Po: The normal atmospheric pressure where the explosion occurred,

- Peak side-on positive overpressure, P_{so}: The maximum value of the overpressure at a particular point,
- Positive phase duration, to: The time taken to decay the positive pressure to ambient pressure,
- Positive impulse, Io: The impulse created by the positive overpressure over a duration, to at the point,
- Peak side-on negative pressure (suction), Pso- : The maximum value of the pressure below the normal atmospheric pressure,
- Negative phase duration, to-: The time over which the pressure is below atmospheric,
- Negative impulse, Io-: The impulse created over the duration, to- at the point

In figure 2.4, detonation occurred at a certain distance away from the building and so the blast wave (pressure wave) took t_A time to arrive. The average pressure surrounding the building was initially P_o which increased instantaneously to a peak pressure P_{so} when the blast wave reaches that point. After its peak value, the pressure decreases with an exponential rate until it reaches the ambient pressure at t_A+t_o, t_o being called the positive phase duration. After the positive phase of the pressure-time diagram, the pressure becomes smaller (referred to as negative) than the ambient value, and finally returns to it. The negative phase is longer than the positive one, its minimum pressure value is denoted as P_{so}^- and its duration as t_o^-. During this phase the structures are subjected to suction forces, which is the reason why sometimes during blast loading glass fragments from failures of facades are found outside a building instead in its interior **[10].**

2.5 Blast Wave Equation

Friendlander's equation is the most widely used equation to describe the decrease in positive incident pressure value with time.

$$P_S(t) = P_{so}\,(1 - \frac{t}{to})e^{-b\frac{t}{to}}$$

Where, P_{so} = peak side-on overpressure

to = positive phase duration of blast

b = decay coefficient of the waveform (non-dimensional parameter)

t = time elapsed, measured from the instant of blast arrival.

$P_s(t)$ = pressure at time t

Given equation gives the expression in the case of the positive phase, which is more significant than its negative counterpart in terms of building collapse prevention. The shaded area under the overpressure-time curve gives impulse which relates to the total force (per unit area) that is applied on a structure due to the blast.

The Indian standard IS 4991-1968 **[8]** provides two equations for calculation of blast load.

$$P_S(t) = P_o\,(1 - \frac{t}{to})e^{-\alpha\frac{t}{to}}$$

$$q_s(t) = q_o\,(1 - \frac{t}{to})e^{-b\frac{t}{to}}$$

The first equation gives the intensity of shock wave with respect to time, constant 'alpha' the decay parameter. Second equation gives the intensity of the dynamic pressure which follows the shock wave front. The dynamic pressure decays faster than the overpressure of the shock wave.

2.5.1. Simplified Blast Wave Profile

Since the use of Friendlander's equation in design problems would involve tedious calculations, the pressure time relation in the positive phase are idealized by using a straight line starting with the maximum pressure value but terminating at a time such that the impulse value remains the same. **[8 , 17].** The simplified blast wave overpressure profile is shown in Fig. 2.5.

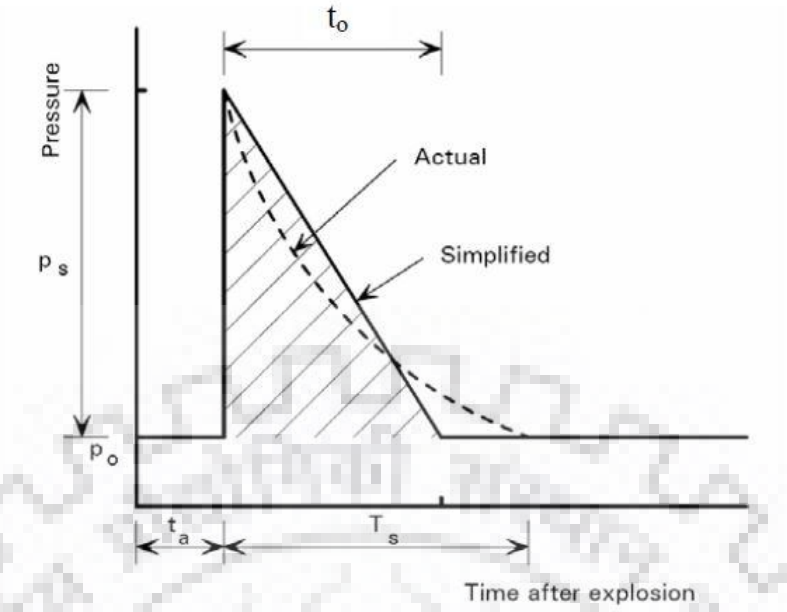

Fig. 2.5: Simplified blast wave overpressure profile [17]

The simplified equation is expressed numerically as,

$$P(t) = P_o + P_s\,(1 - \frac{t}{t_o})$$

2.6 Scaling Effect and Scaled Distance

The response of a structure to blast loads depends on its location relative to the source of the explosions. This distance is called the **stand-off distance [14]**. Scaling laws have been introduced to identify the properties of blast waves in terms of charge weight and standoff distance. This law states that similar blast waves are generated at an identical scaled distance.

$$Z = \frac{R}{W^{\frac{1}{3}}}$$

Here, Z = Scaled distance

R = standoff distance

W = mass of spherical TNT charge equivalent

2.7. Dynamic Pressure

Apart from the incident overpressure-time profile created by blast, there is another shock wave formed which follows the explosion called dynamic pressure. Dynamic pressure is associated with the wind behind the shock front. It is a function of air density and wind

velocity. This peak dynamic pressure q_o is determined by an empirical formula developed by Newmark for the low overpressure range with normal atmospheric conditions. **[9]**

$$qo = \frac{2.5\ {P_{so}}^2}{(7P_o + P_{so})}$$

2.8. Structural Response to Blast Loads

A structure subjected to blast loads experiences sudden changes in stress and strain **[9]** having very small time durations in the range of milliseconds. Under normal loading conditions such as superimposed dead, live or wind loads structures can behave in elastic range. However, during blast analysis and design the yielding and plastic behaviour of the structure must be incorporated. The structure exhibits global and local failure. The main global failure mode of reinforced concrete structures is the Bending failure while shear failure is treated as a secondary global failure caused by high intensity blast pressures directly applied to the critical region of a structure. On the other hand, the local structural response of a concrete member could have ductile or brittle mode which exhibits failure modes like direct spalling of concrete, scrabbing, bleaching etc.

2.9. Material Response to Blast Loads

Under blast loads, due to rapid loading environment, material behaves significantly different than under static loading conditions. This is due to the material's inability to rapidly deform beyond the normal rate in static loading **[9].** Thus, the yielding stress of the material increases due to strain hardening. Consequently, a structural member gains additional strength enhancement in excess of its static loading conditions. Strain rates under typical blast loading varies in the range of 10^2-$10^4 s^{-1}$. Figure …….demonstrates strain rates variation for several loading conditions.

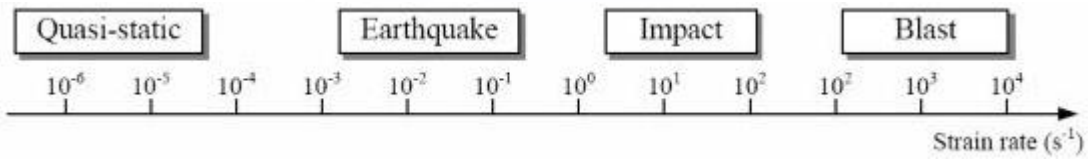

Fig 2.6 : Strain rates for different loading conditions [9]

Table 2.2: Dynamic Increase Factor (DIF) for design of RCC [12]

Stress	Concrete	Reinforcing Bars	
	f_{dcu} / f_{cu}	f_{dy} / f_y	f_{du} / f_u
Bending	1.25	1.20	1.05
Shear	1.00	1.10	1.00

CHAPTER 3

RESPONSE OF MULTI-STOREY REINFORCED CONCRETE FRAME STRUCTURES SUBJECTED TO DISTANT EXPLOSIONS

3.1. Introduction

The relative distance of the detonation center with the target structure as well as the size of the structure itself results in two classes of blast wave surface interaction.

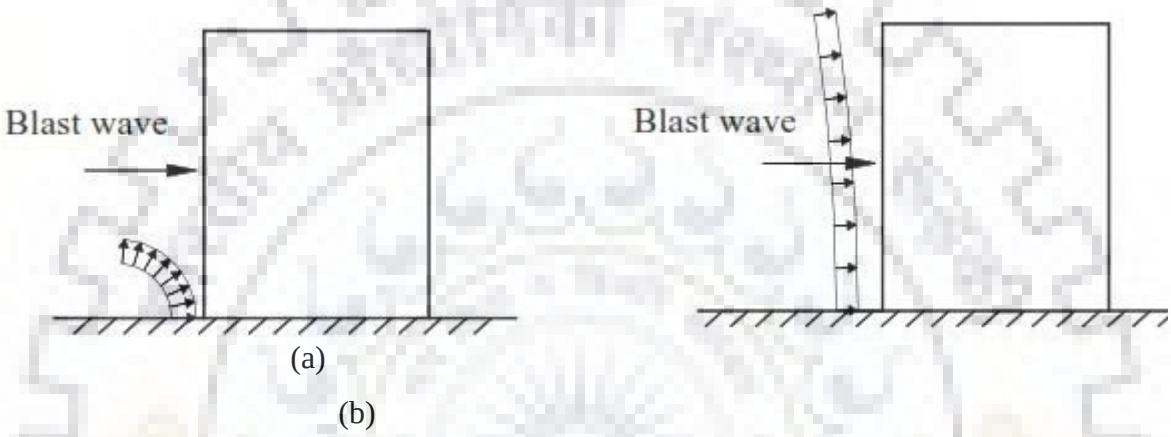

Fig 3.1.: Two classes of blast wave-surface interaction [4]

Fig. 3.1(a), the first class shows the interaction of a blast wave produced by the detonation of a smaller charge loading a target structure at a short standoff distance. This usually happens for most terrorist attacks such as car bombings. Here, the blast pressures are produced locally to individual structural members and the members are likely loaded sequentially. This causes excessive local failure of several critical structural members followed by progressive collapse. Fig 3.1(b), the second class shows the interaction of a blast wave on a relatively distant structure. This happens due to accidental severe surface explosion of petroleum refineries, chemical plants and ammunition storage areas, fuel train explosions, or nuclear devices of substantial yields, and so on. Here, a normal squashing force will be applied to every exposed surface and this tends to move the structure body laterally **[4]**.

Many explosion tests and numerical analyses have been carried out to analyze the behaviour of first class structures, however for the second class, the literature available is limited. Now it is true that the explosions resulting in the second class of blast wave-structure interaction

are very rare, it is also true that when such explosions do happen the consequences are severe, more so upon structures which are not specifically designed to withstand such pressures.

By simplifying the members and the structural system into equivalent single-degree-of-freedom (SDOF) systems, Biggs **[1]** provided a blast resistant design procedure for one-storey structures using Ductility as performance indicator and May & Smith provided its procedure using Displacement as performance indicator. However, very limited research is available for multi-storey reinforced concrete (RCC) frame structures, mostly common to civilian building.

3.2 Design of the Target Frame Structure

To study the dynamic behaviour of frame structures under distant blast loading, a 3-D six-storey RCC structure is designed. The loads involved are Dead load, Live load, Super-imposed dead load and blast dynamic loads. The layout of the structure is shown is Fig. 3.2. Two blast waves produced by a detonation equivalent to 80 tonne TNT (blast condition I) and 30 tonne TNT (blast condition II) at ground level with a standoff distance of 100 m is considered in this study. Due to symmetry of both, the configuration of structure and the blast pressure distribution on it, a cross-section is taken out and modelled to simulate the whole structural dynamic response.

This 3-D building has cladding at the front of the building which is made of reinforced concrete having a thickness of 150 mm having sufficient out-of-plane strength and stiffness to prevent the blast waves from entering the building together with floor slabs, beams and columns. Thus the building is modelled as a closed frame rather than a bare frame. The modelling of the structural responses have to include the exterior infill walls / cladding panels together with the floor slabs, beams and columns.

Since the 6-storey building taken is symmetrical about the length and width, instead of analyzing the entire 3-D building in ETABS due to blast load, a cross – section is cut in the form of a 2-D reinforced concrete frame. The design calculations are now carried out on this 2-D RC frame. Figure 3.2 below shows the structural layout and the elevation plan of the building.

The 3-D building has 6 storeys having the total length of 24 m, width of 18 m and the total height of 22.2 m. The bottom two storeys are 4.5 m each and the above 4 floors are 3.3 m. The concrete dynamic compressive strength is taken as 40 MPa and the longitudinal reinforcement dynamic yield strength is taken as 520 MPa.**[7]**

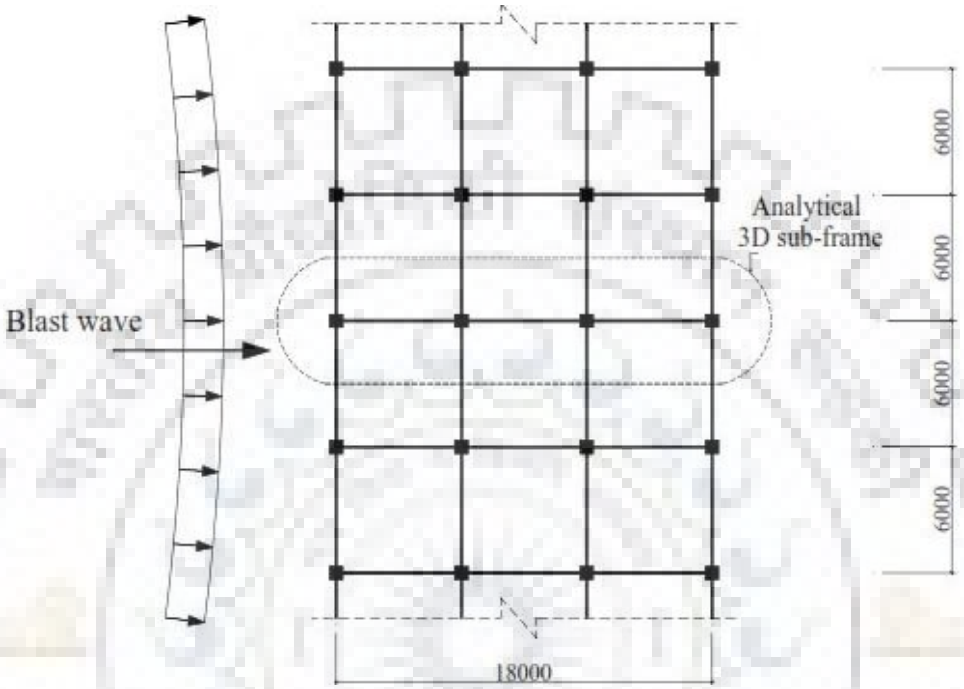

a) Structural Layout

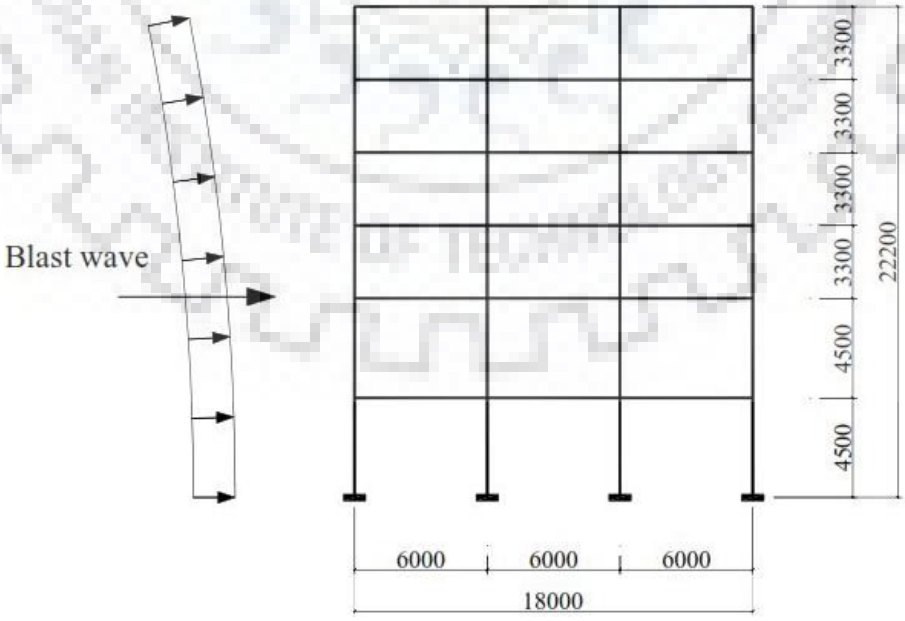

b) Elevation view

Fig. 3.2: Details of the target six-storey frame structure

3.3 Blast Load Calculations

Blast load parameters can be obtained from charts provided in the literature **[16 , 17]**. In general, the properties of the blast waves are expressed in terms of a scaled distance, *Z*. Well known standard charts and equations are presented in TM5-1300, for blast load estimations for conventional analysis. Figure 3.3 shows the standard chart provided by Figure 2-15 in TM5-1300 to determine blast load parameters.

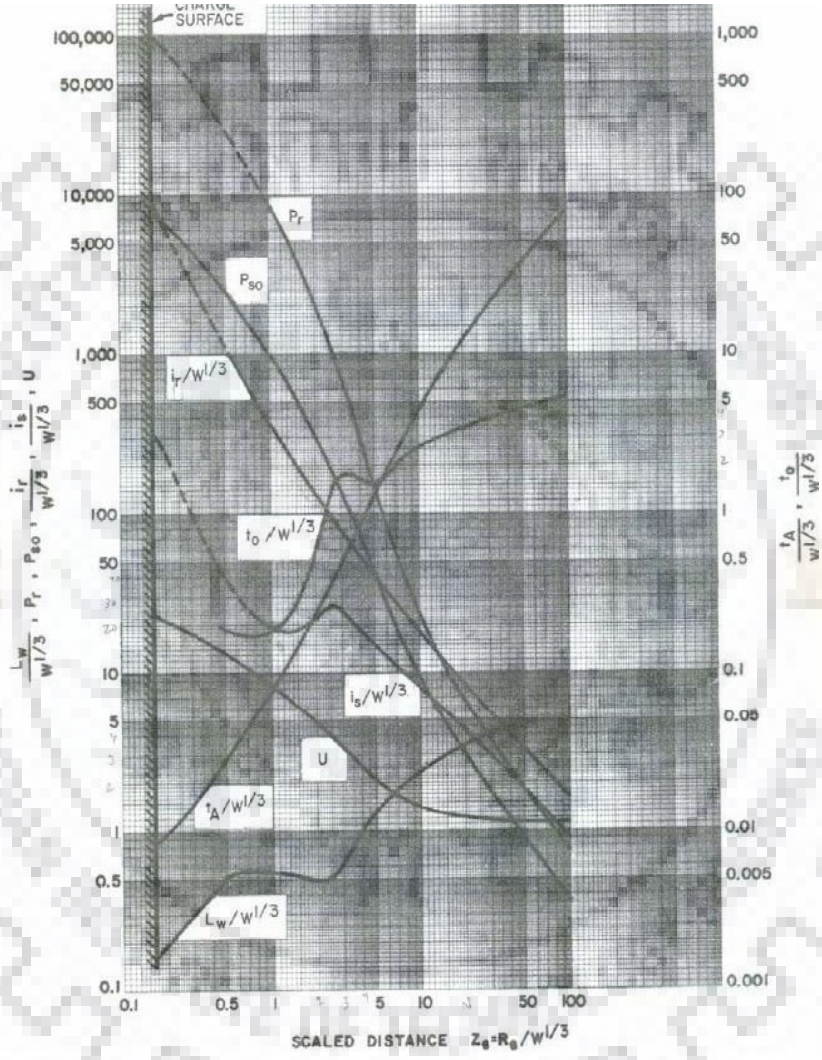

Figure 3.3: Positive phase shock wave parameters for a hemispherical TNT explosion on the surface at sea level [TM5-1300 1990, Figure 2-15]

3.4. Blast Loadings on various sides of structure

As blast wave strikes various sides of the structure at different angles, different sides experience different pressure intensity with various duration **[9]**. Since the standoff distance is very high compared to the height of the building for our analysis, the blast pressure can be assumed to act as planar wave on the frame. Figure 3.4 below shows the positive pressure acting on the front face of the building and a suction acts on the roof top and the rear face

of the building. The blast load calculations on these faces are calculated using IS 4991-1968 as shown and categorized below on a typical structure:

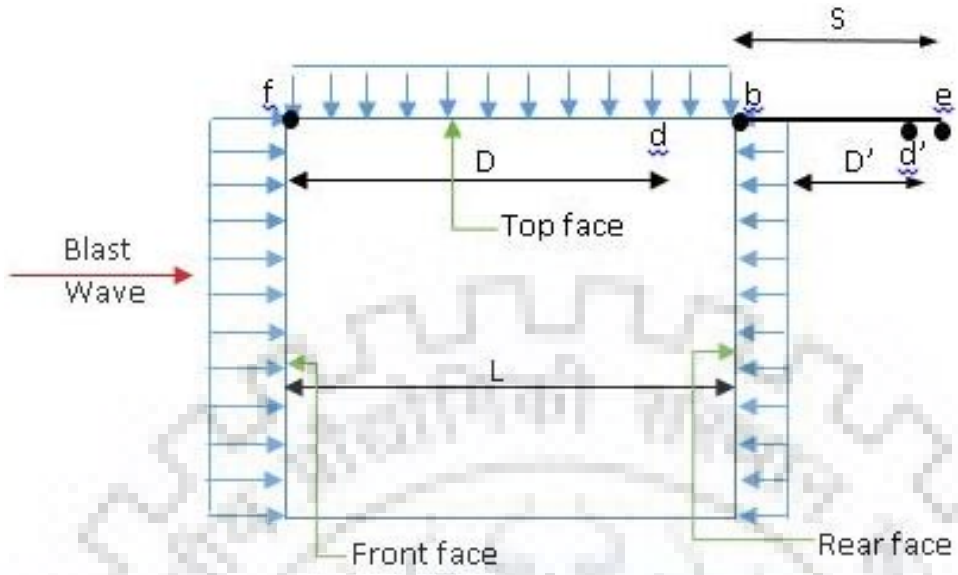

Fig.3.4: Blast dynamic pressure causing push on front face of target followed by suction force on top and rear as blast waves pass over and round the target [16]

3.4.1: Front face loading

This is the surface which is first hit and is normal to the direction of propagation of the blast wave. When the explosion occurs on the surface, the pressure generated gets reflected from the ground making it rise, thus becoming over-pressure. As this wave travels further and hits the front face, a reflection of incoming wave again occurs from the surface. This reflection causes considerable increase in peak over pressure due to constructive interference of the incident and the reflected waves, therefore the pressure further rises in magnitude called the reflected over pressure. This reflected over pressure acts only till the clearance time, t_c .

$$t_c = \frac{3S}{U} \text{ or } t_{eq}, \text{ whichever is less} \qquad \text{[IS: 4991-1968]}$$

Where, S = H or B/2 whichever is less

U = shock front velocity

After clearing time, t_c , $P = P_s + C_d\, q$ [IS: 4991-1968]

Where , Ps = incident pressure

q = dynamic pressure

C_d = 1 (for vertical front face)

3.4.2. Side face and top face (Roof) loading

Side faces are vertical surfaces of the structure which are parallel to the direction of propagation of shock wave. Structure is symmetric, thus the side face pressure cancels each other.

The top surface (roof) is the horizontal surface of the structure which is parallel to the direction of propagation of shock wave. When shock front passes over the top face, it moves parallel to the surface and no reflection of incident waves takes place. The peak pressure acting on the surface is the sum of contributions of equivalent uniform shock pressure and drag pressure.

$$p_r = C_E.P_{sof} + C_D \,.q_{of}$$

Where C_E = equivalent load factor (function of P_{sof})

P_{sof} = peak incident pressure at front edge

C_D = drag coefficient

q_{of} = peak dynamic pressure at the front edge

Table 3.1: Drag coefficient for Top surface at various Dynamic Pressures [IS 4991-1968]

Peak dynamic pressure (kg/cm^2)	Drag Coefficient
0.0 – 1.8	- 0.40
1.8 – 3.5	- 0.30
3.5 – 9.0	- 0.20

3.4.3. Rear face loading

Rear face is not hit by shock waves directly, but generated as secondary waves or spilled over from the top face (roof) and side faces.

$$p_r = C_E.P_{sob} + C_D \,.q_{ob}$$

Where C_E = equivalent load factor (function of P_{sob})

P_{sof} = peak incident pressure at middle point of rear edge

C_D = drag coefficient (same as top face)

q_{ob} = peak dynamic pressure at middle point of rear edge

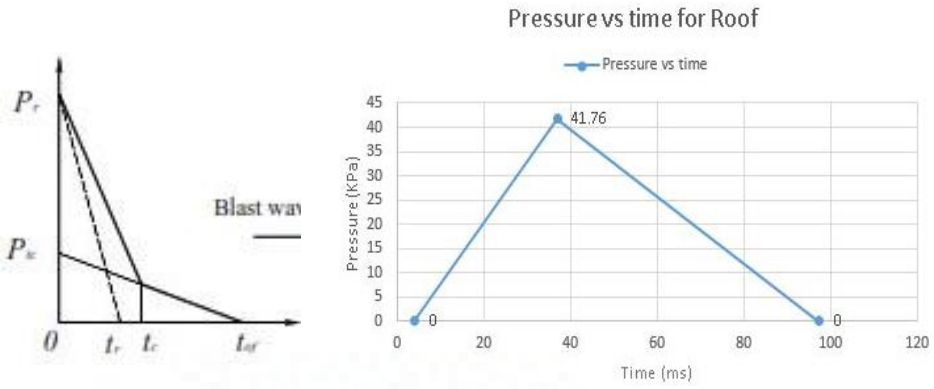

a) Front face b) Top face

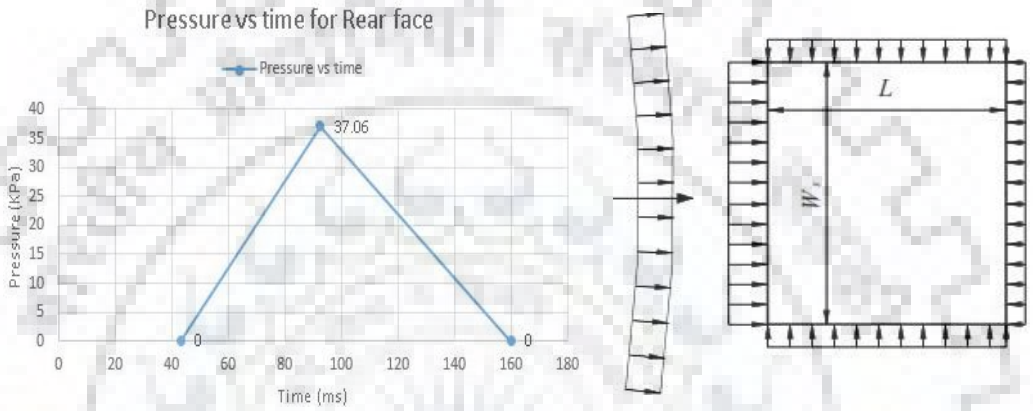

c) Rear face d) Side face

Fig.3.5: Blast loading on various sides of structure

3.5. Material Modelling

The modelling is done in ETABS-2015. The stress-strain plot for concrete is modelled using Mander model which is inbuilt in ETABS while no special modelling is provided for steel reinforcement.

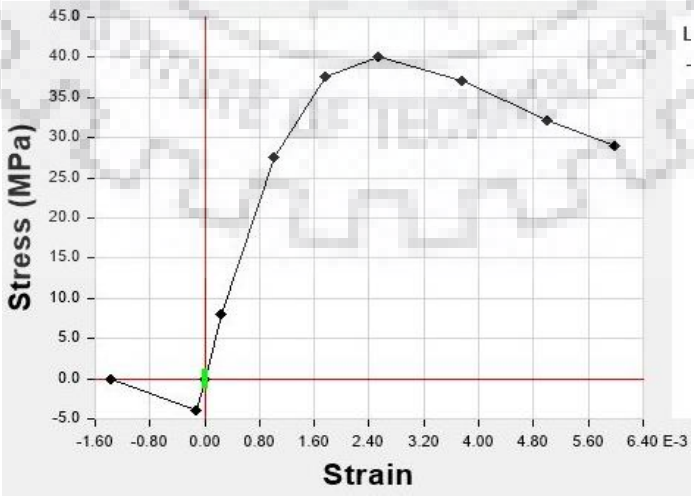

Fig 3.6: Stress-strain plot for Concrete M40 [Mander model]

3.6. Hinge Properties

The post yielding behavior is modelled using discrete user-defined hinges. Plastic hinges affect the behaviour of the structure in non-linear static and nonlinear time-history analysis. Hinges are taken as Idealized bilinear moment-curvature curves using **FEMA-356**.

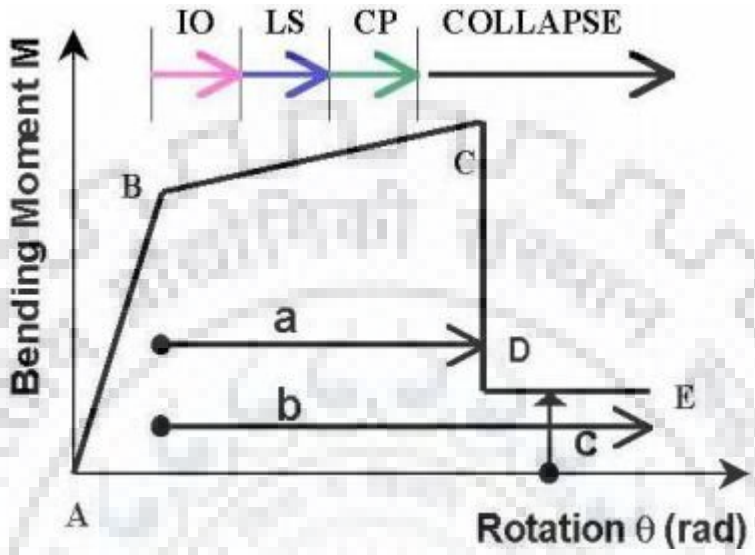

Fig 3.7: Plastic Hinge Model per FEMA-356 (IO = immediate occupancy, LS = life safety, CP = collapse prevention)

The beam hinge taken is a ductile deformation controlled Moment hinge. Since, the blast distance is far, the entire frame undergoes a global deformation that tilts the building towards the direction of the blast. Had, it been a near blast causing sequential loading, shear hinge could have been formed before moment hinge but not here.

The column hinge is a ductile deformation controlled Interacting P-M2-M3 curve. The hinge length is taken as per **FEMA-356** which provides for a usual length of half of the thickness of the frame member. The collapse prevention moment is taken as 1.10 x yield moment corresponding to which the curvature is found out. Similarly, the life safety curvature is taken corresponding to 0.8 times the collapse prevention curvature and the immediate occupancy curvature is taken as 0.2 times the collapse prevention curvature.

CHAPTER 4

PERFORMANCE-BASED BLAST RESISTANT DESIGN OF SINGLE DEGREE OF FREEDOM SYSTEM (SDOF) WITH EQUIVALENT STATIC FORCE (ESF)

4.1 Introduction

Based upon relative distance of explosion with target structure and size of the structure, there can be generally two types of blast wave-structure interaction. First type of interaction of blast wave is produced by the detonation of a smaller charge loading target structure up to a short height from base of the structure. However, the second type of interaction is due to a relatively distant structure which might be present due to an accidental surface explosion of petroleum refineries, chemical plants or nuclear devices **[3 , 13]**. In such a situation, the structure is subjected to the uniform loading at all levels up to its height. This type falls under the category of distant blast loading. The reinforced concrete members subjected to distant blast loading may sustain severe damages but with provision of additional reinforcement in appropriate positions, the structure might withstand the blast more effectively resulting reduced level of damage. In view of this, it is very important to study various aspects related to analysis of structures under distant blast loading. In view of the difficulty in handling the blast forces with short durations on structures, generally, the dynamic forces are transformed into equivalent static forces (ESF) and then the analysis is carried out **[5 , 6 , 7]**. This has been proved to be a reliable way of analyzing the structures under dynamic loads as these produce an equivalent response of the structures.

Single degree of freedom (SDOF) systems are often employed for dynamic analysis of broad range of structures where the first mode of vibration is responsible for the overall structural behavior. Dynamic analysis of such a SDOF system was carried out many research workers and now is a part of the standard literature **[1 , 12 , 15]**.

Simple ready to use non-dimensional design charts are also available for the response of SDOF systems under various types of dynamic loading conditions.

Performance based design concept include the fact that the design should be able to ensure the damage of the structure within a certain limit. This permissible limit is defined as the performance level which is usually specified in terms of displacement, displacement ductility factor or the drift ratio with reference to the structure subjected to dynamic loading conditions. It is generally advantageous, economically and structurally, to allow plastic deformation of structures subjected to distant explosions in view of its extremity and lesser probability of occurrence. Therefore, the constitutive relationship of the material is assumed to be elasto- plastic.

Basically the design method developed with ESF is for the design of a RC frame structural system in controlling its MIDR response, which occurs at a time generally later than the blast loading duration (t_d) **[5 , 6].** The descriptions of the model of ESF and the design method with ESF for a SDOF system herein are only to provide a theoretical basis. Therefore the assumption that the peak response (maximum displacement for a SDOF system or MIDR for a frame structure) takes place after the loading duration t_d is generally adopted in the study.

4.2 ESF for a SDOF System

4.2 1 Process for the construction of ESF

Because of the short duration of the blast loading, the vibration of a SDOF system after reaching the peak response will be limited within its elastic range inducing no further cumulative damages **[1]**. Therefore for a well-defined SDOF system, the maximum displacement response can adequately characterize its damage status in blast events. Under such conditions, if there exists a force, which makes it possible for the SDOF system to experience exactly the same maximum displacement response when statically applied, this force is called the equivalent static force (ESF) of the blast loading. To calculate the ESF of the blast loading on a SDOF system, a model is presented herein with its process plotted in Figure 4.1.

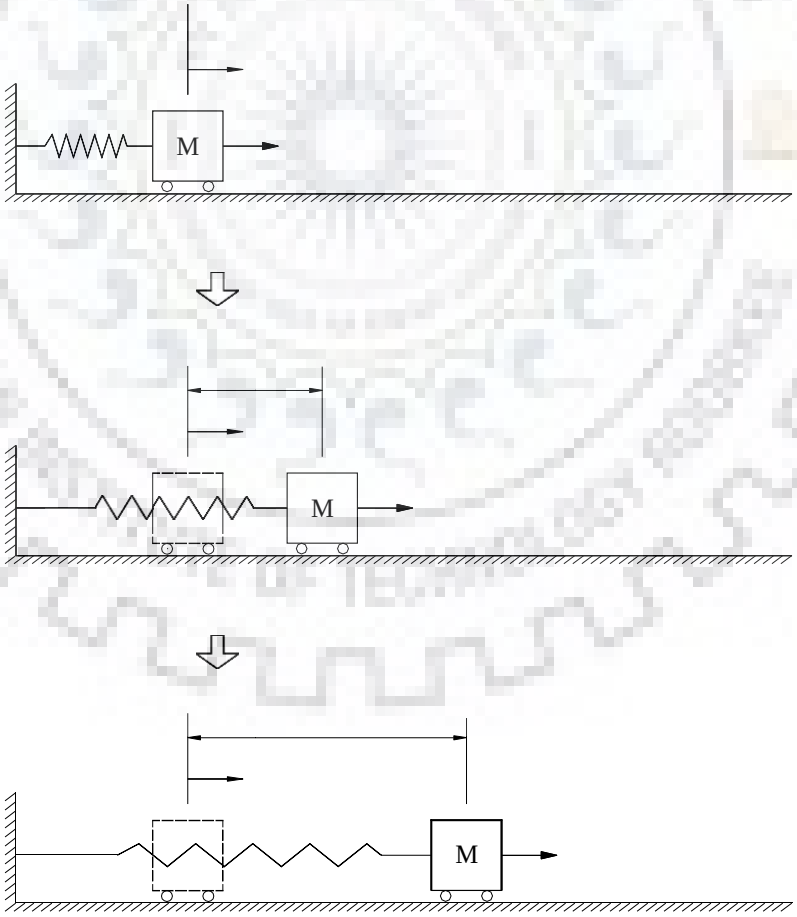

Figure 4.1 (a). Dynamic response process of the original SDOF system under the blast force

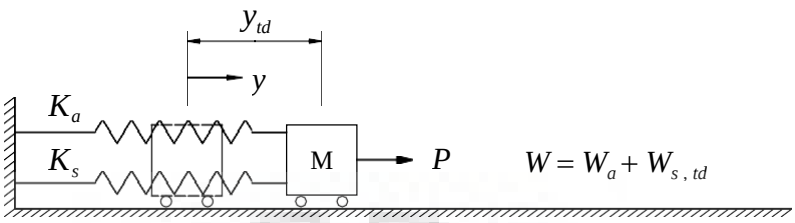

(b). Equivalent static system

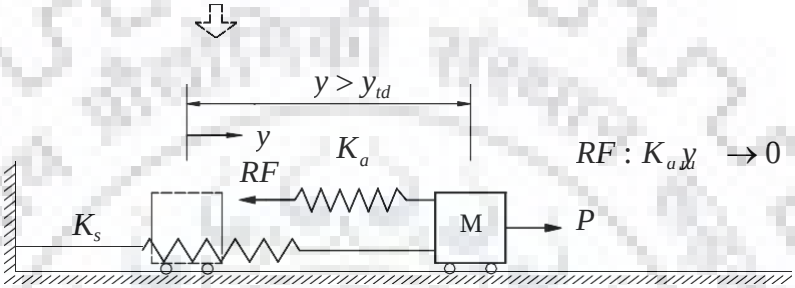

(c). Releasing the strain energy in spring K_a

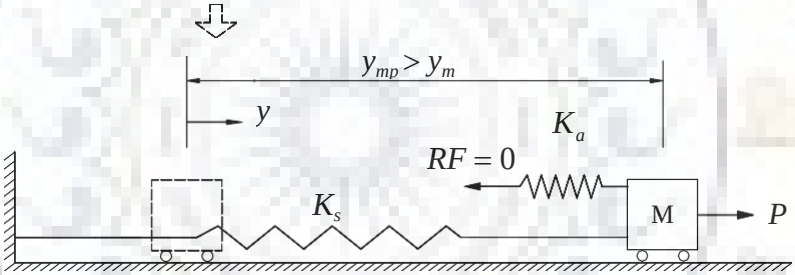

(d). Recovering to the original SDOF system plus the action of P

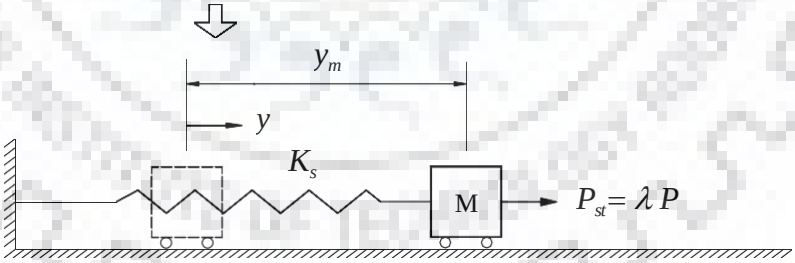

(e). Equivalent static force

Figure 4.1 Process for the construction of ESF for a SDOF system

The blast force can be reasonably simplified into a triangular pulse only if the peak pressure and impulse are preserved, hence the function of the blast force is written as

$$F(t) = \begin{cases} F_1(1 - t/t_d) & t \le t_d \\ 0 & t > t_d \end{cases} \tag{4.1}$$

where t_d is the duration and F_1 is the peak amplitude of the blast force. Since after t_d, the blast force will keep zero, no additional external energy is produced and the total energy within the SDOF system consisting of the kinetic energy and the strain energy will keep constant whose magnitude determines the maximum response by ignoring the damping effects. The constant total energy can be obtained from the response state of the system at t_d plotted in Figure 4.1a, written as

$$W = W_{k,td} + W_{s,td} \tag{4.2}$$

where W is the constant total energy of the SDOF system; $W_{k,td}$ and $W_{s,td}$ are the kinetic and strain energy at the time t_d respectively. In order to simulate the energy components of the SDOF system equally at this time step, an equivalent static SDOF system is constructed as shown in Figure 4.1b, where an additional elastic spring is added to the original SDOF system. It is proposed that under a certain external static force P, the equivalent static system experience the same displacement response as y_{td} (the dynamic response of the original SDOF system at t_d) and therefore the strain energies within the spring K_s in both systems are identical. In order to model the kinetic energy, the strain energy W_a within the additional spring K_a should be equal to $W_{k,td}$, thus

$$M \dot{y}_{td}^2 / 2 = K_a y_{td}^2 / 2 \tag{4.3}$$

and

$$K_a = M \dot{y}_{td}^2 / y_{td}^2 \tag{4.4}$$

where $\dot{y}_{td}$ is the velocity of the original SDOF system at the time of t_d under $F(t)$, K_a is the elastic stiffness of the additional spring. From the equilibrium of the equivalent static system

$$P = F_s + F_a = F_s + K_a y_{td} = F_s + M \dot{y}_{td}^2 / y_{td} \tag{4.5}$$

where F_s and F_a is the force produced respectively by the original and additional spring (K_s and K_a) in the equivalent static system in Figure 4.1b.

After t_d, the kinetic energy $W_{k,td}$ will be gradually transformed into the strain energy causing further displacement for the original SDOF system until the maximum response y_m is reached as shown in Figure 4.1a. For modelling this process with the equivalent static system, the strain energy W_a in the additional spring K_a needs to be released statically in such a way that this part of energy is transferred to the original spring K_s as shown in Figure 4.1c. With the support of the additional spring statically moving toward the spring until the support reaction force RF decreases to zero, the equivalent static system is recovered to the original SDOF system with the static force P exerting on it in Figure 4.1d. However it should be noted that during this process, an amount of extra positive external energy is produced by P together with the declining RF ; and a relatively larger displacement response y_{mp} will be induced than y_m for the original SDOF system under the blast condition. Thus an ESF factor (λ) less than one is applied to P producing the ESF (P_{st}) that creates the same maximum response as y_m when statically applied to the original SDOF system as shown in Figure 4.1e

$$P_{st} = \lambda P \tag{4.6}$$

4.2.2. ESF factor

For a SDOF system with the elastic-perfectly-plastic resistance function, the close form solution of the ESF factor λ is derived with respect to three different cases according to the response states at the time t_d and t_m (the time for maximum displacement response) as plotted in Figure 4.2. They are

- Case I : in the elastic state at $t = t_d$ as well as $t = t_m$;
- Case II : in the elastic state at $t = t_d$ while in the plastic state at $t = t_m$;
- Case III: in the plastic state at $t = t_d$ and $t = t_m$.

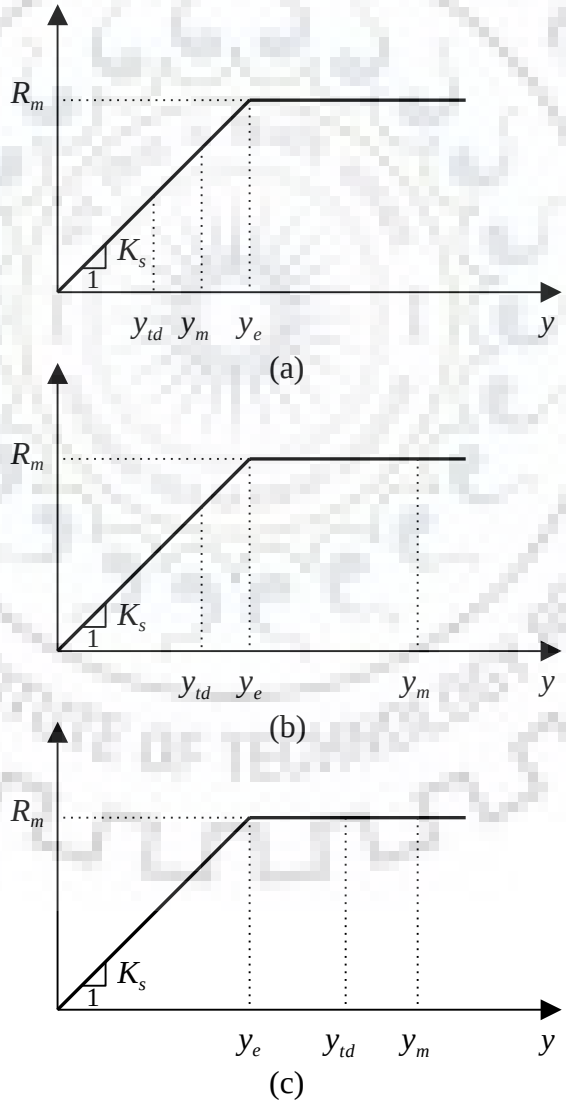

Figure 4.2 Three different response states for a SDOF system at the time t_d and t_m

Case I: In this case, since the SDOF system is still within its elastic limit during the whole response process as shown in Figure 4.2a, the constant total energy at t_d and t_m can be written as

$$W = K_s \; y_{td}^2 / 2 + M \; \dot{y}_{td}^2 / 2 \tag{4.7}$$

and

$$W = K_s \; y_m^2 / 2 \tag{4.8}$$

where K_s is the initial stiffness of the elastic-perfectly-plastic SDOF system. Equating Equations (4.7) with (4.8) leads to

$$M \; \dot{y}_{td}^2 = K_s \; (y_m^2 - y_{td}^2) \tag{4.9}$$

Subjecting Equation (4.9) into Equation (4.5) and considering that the spring K_s is in its elastic range at t_d

$$P = K_s y_m \frac{y_m}{y_{td}} \tag{4.10}$$

To meet the requirement that the same y_m appear for the SDOF system under the ESF, P_{st} should be equal to its resistance at the displacement y_m, which in the elastic range is given as

$$P_{st} = K_s y_m \tag{4.11}$$

Substituting Equations (4.10) and (4.11) into Equation (4.6), the ESF factor λ in this case is determined as

$$\lambda = \frac{y_{td}}{y_m} \tag{4.12}$$

Case II: For the second case, where the SDOF system has entered the plastic response stage, Equation (4.8) for the calculation of the constant total energy at t_m changes into

$$W = \frac{1}{2} K_s y_e (2y_m - y_e) \tag{4.13}$$

where y_e is the elastic limit displacement of the SDOF system. Equating the Equations (4.7) with (4.13) obtains

$$M \ddot{y}_{td}^2 = K_s (2 y y_m - y_e^2 - y_{td}^2) \tag{4.14}$$

By subjecting Equation (4.14) into Equation (4.5) and considering that the spring K_s is in its elastic range at t_d, P is given as

$$P = K_s y_e \frac{(2 y_m - y_e)}{y_{td}} \tag{4.15}$$

In order to statically produce the same maximum displacement as y_m in the blast condition, which is beyond the elastic limit of the SDOF system with elastic perfect plastic resistance function, the ESF (P_{st}) should be identical with the ultimate strength, thus

$$P_{st} = K_s y_e \tag{4.16}$$

The value of λ is finally obtained by subjecting Equations (4.15) and (4.16) into Equation (4.6) as

$$\lambda = \frac{y_{td}}{2 y_m - y_e} \tag{4.17}$$

Case III: Since the SDOF system has entered its plastic response stage before t_d, W for the elastic-perfectly-plastic SDOF system at t_d is given by

$$W = \frac{1}{2} K_s y_e (2y_{td} - y_e) + \frac{1}{2} M \dot{y}_{td}^2 \tag{4.18}$$

In this case, Equation (4.13) is also valid for expressing W at t_m, therefore equating Equations (4.13) with (4.18) brings out

$$M y_{td}^2 = 2K_s y_e (y_m - y_{td}) \tag{4.19}$$

By taking $F_s = K_s y_e$ and subjecting Equations (4.19) into Equations (4.5), P is gained as

$$P = K_s y_e \frac{(2y_m - y_{td})}{y_{td}} \tag{4.20}$$

With Equation (4.16) for the evaluation of P_{st}, λ is derived from Equations (4.6) and (4.20) as

$$\lambda = \frac{y_{td}}{2y_m - y_{td}} \tag{4.21}$$

4.3. Calculation model for ESF

By summarizing the above analyses, a model to calculate the ESF for an elastic-perfectly-plastic SDOF system is presented in Equation (7.22). An extra variable X is introduced, which is for the convenience of extending this model to multi-storey reinforced concrete frame structures as discussed in Chapter 5. Obviously there is a 45^o linear relationship between λ and X as shown in Figure 4.3. The physical

meanings for the other variables have been well defined previously.

$$\begin{cases} P_{st} = \lambda P \\ P = F_s + F_a \\ \lambda = X \\ X = \begin{cases} y_{td} / y_m & y_m \le y_e \\ y_{td} /(2\, y_m - y_e) & y_{td} \le y_e \text{ and } y_m \ge y_e \\ y_{td} /(2 y_m - y_{td}) & y_{td} \ge y_e \end{cases} \end{cases} \tag{4.22}$$

It should be pointed out that this model does not attempt to calculate the ESF with the purpose of assessing the maximum response of a particular SDOF system under the blast condition, but provides a powerful tool in designing the ultimate strength of the system to achieve the target of the displacement response. The design method based on this model is addressed in the following section.

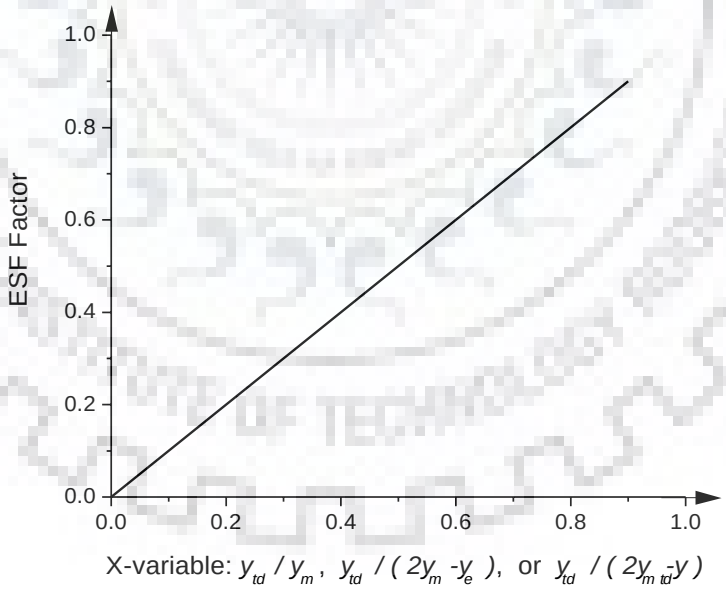

Figure 4.3 Distribution of the ESF factor for the SDOF system

CHAPTER 5

PERFORMANCE-BASED BLAST RESISTANT DESIGN OF MULTI-STOREY REINFORCED CONCRETE FRAME STRUCTURES WITH EQUIVALENT STATIC FORCE (ESF)

5.1 Introduction

While designing multi-storey RCC frame structures for a distant blast loading, a significant global failure may occur due to high Inter-storey Drift thereby causing a certain degree of global damage. Therefore, controlling their maximum inter-storey drift ratio (MIDR) responses becomes an important consideration.

Drift is defined as the lateral displacement. Storey-drift is the drift of one level of a multi-storey building relative to the level below. Inter-storey drift ratio is defined as the difference between the roof displacement and the floor displacement of a storey divided by the height of the particular storey. The values of inter-storey drift ratio and the corresponding response levels and damage degrees is provided in Table 4.1.

Table 5.1: Inter-storey drift Ratio vs Damage [2]

Response Level	Inter-storey drift ratio	Damage description
Low	**1/50 (2%)**	**Localized building/component damage**
Medium	**1/35 (2.86%)**	**Widespread building/component damage**
High	**1/25 (4%)**	**Building/component losing structural integrity and having possibility of collapse due to environment condition**

Blast loads act dynamically on structure and the dynamic loadings are very difficult to handle within the structural design since they cannot be directly implemented to calculate the interior forces of the structural members. In designing a building to resist seismic/wind loads, the dynamic seismic/wind actions are usually transformed into the static loadings, which are deemed to be able to produce equivalent effects on structures **[4]**. Along similar

lines, if an equivalent static force (ESF) can be applied to the structure that could closely represent the effects of the distant blast loadings, it will highly facilitate the blast design.

Blast loading duration being very small, the peak response (MIDR for a frame structure) usually takes place after time $t_{d,}$ the duration for which blast load acts on the structure.

5.2 Process for the development of ESF for a multi-storey frame

For a frame having n storeys, we define ESF (P_{st}) as a column vector of point force, which, when applied statically to each floor level, will produce the same MIDR that is being produced by a blast load.

Thus, $P_{st} = \{P_{st,1} , P_{st,2} , \ldots\ldots, P_{st,n} \}^T$

Here, $P_{st,i}$ = component of ESF at i^{th} floor level

Fig……..shows the process of evaluation of $P_{st.}$. Blast load acts for a duration t_d, at the end of which, the frame structure acquires displacement and velocity as shown in Fig…..

Here, $y_{td} = \{ y_{td,1} , y_{td,2} , \ldots\ldots, y_{td,n} \}^T$, $y_{td,i}$ is the i^{th} floor displacement at time t_d.

After time t_d when the blast load stops acting on the frame, the kinetic energy acquired as a function of the velocity will be gradually transformed into further deformation till it reaches the MIDR (Δ_m) as shown in Fig…..

Now, to obtain an equivalent static system as shown in Fig……, the kinetic energy $W_{k;i}$, which represents the kinetic energy within the part of the frame located halfway above and below the i^{th} floor level at time t_d, is transformed as the strain energy $W_{a,i}$ of an additional uncoupled spring $K_{a;i}$ at the corresponding floor level having the same deformation as $y_{td;i.}$

For the additional uncoupled spring,

$$W_{a,i} = \frac{1}{2} K_{a,i} {y_{td}}^2 = W_{k,i} = \frac{1}{2} M_i {v_{td}}^2$$

$$K_{a,i} = \frac{2 W_{k,i}}{{y_{td,i}}^2}$$

$K_{a,i}$ = stiffness of the additional elastic spring at the i^{th} floor level. To maintain equilibrium under equivalent static system, the external static force

$P = F_s + F_a$

$P = \{P_1 , P_2 , ….., P_n\}^T$: external static force

$F_s = \{F_{s,1} , F_{s,2} , ….., F_{s,n}\}^T$: resistive force of frame corresponding to deformation of y_{td}.

$F_a = \{F_{a,1} , F_{a,2} , ….., F_{a,n}\}^T$: resistive force of frame corresponding to additional elasitic springs at deformation of y_{td}, where $F_{a,i} = K_{a,i} y_{td,i}$

Therefore, $F_{a,i} = \frac{2W_{k,i}}{y_{td,i}}$

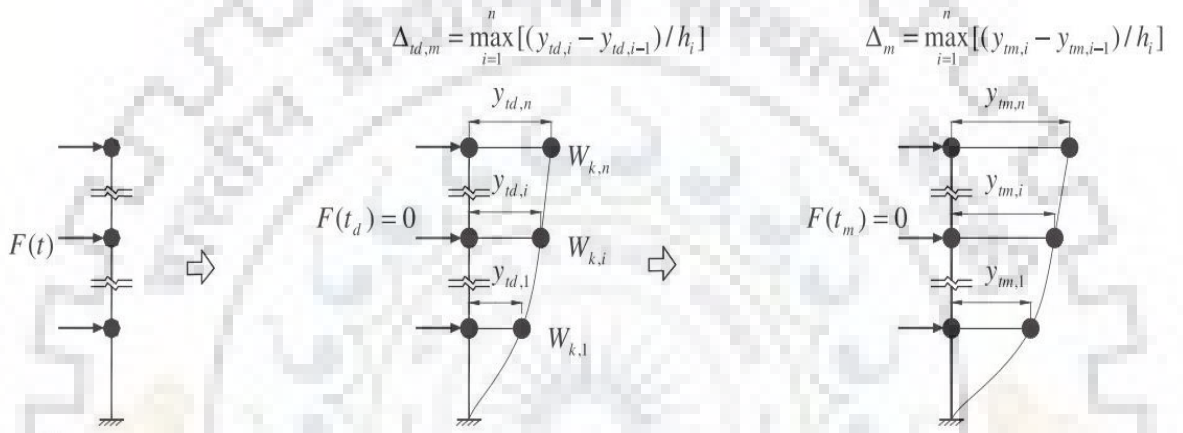

a) Dynamic Response under blast force

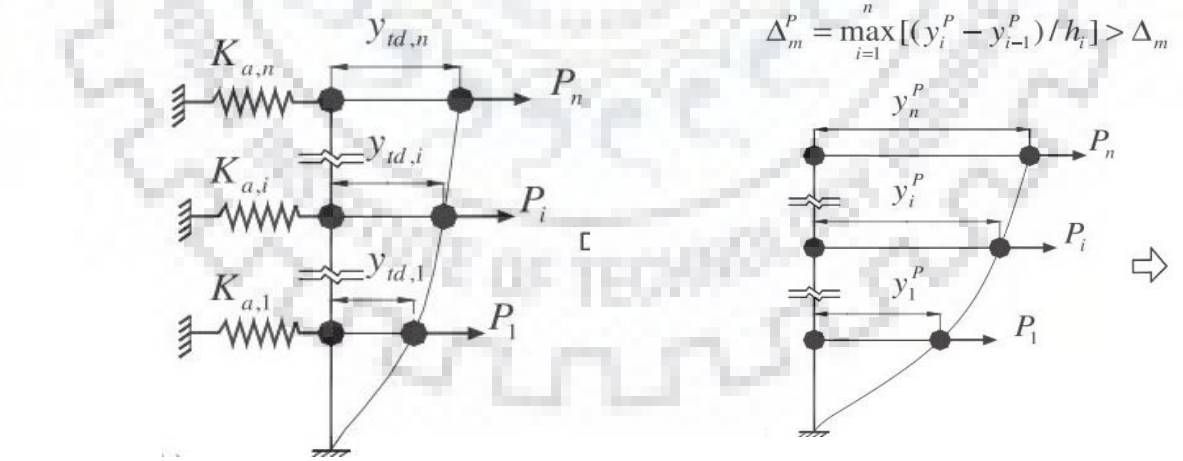

b) Equivalent Static system

c) Static response under P

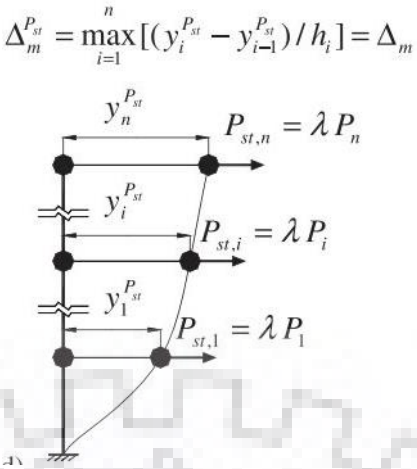

d) Static response under P_{st}

Fig. 5.1: Process for ESF construction for an RC frame structure

To further simulate the transformation of kinetic energy into further deformation after t_d, strain energy within springs $K_{a,1}$, $K_{a,2}$, ……$K_{a,n}$ is released statically in a manner that their supports move towards the springs til the equivalent static system goes back to the original frame structure with P acting on it. However, due to the extra positive external work produced by P, a larger MIDR will be induced in this way than that of the frame structure under the blast loading (Δ_m) as shown in Fig.(c). Thus, an ESF factor λ is introduced to decrease P such that the ESF (P_{st}) is produced, which creates the same MIDR as Δ_m when statically applied to the original frame structure as shown in Fig. 1(d)

$$P_{st} = \lambda P$$

5.3 Procedure to obtain λ

To obtain λ, we compare the MIDR of a RC frame structure under blast loading with the corresponding nonlinear static pushover analysis of the structure under the force P. In pushover analysis, Load control is used wherein, structural loading is applied incrementally in accordance with a certain predefined pattern of the lateral load vector P. The step is mentioned below:

1. Analyze a frame structure with a blast loading acting on it.

2. Evaluate $y_{td,i}$, $W_{k,i}$ and Δ_m, the MIDR within the whole dynamic response process, using nonlinear dynamic time-integration analysis.

3. Calculate the recovery force $F_{a,i}$ by applying $y_{td,i}$ to the structure through nonlinear static analysis.

4. Compute the external static force P.

5. Carry out the nonlinear pushover analysis of the frame structure as Load control under a gradually increasing load vector distributed as P.

6. Plot the curves obtained for load versus the inter-storey drift responses for different storey levels, and find the value of λ at the critical storey level whose inter-storey drift ratio firstly reaches the value of Δm under the gradually increasing force of P.

The empirical analysis was carried out by Li and Rong (2006b) for which 30 samples were chosen to find the value of λ.

Therefore, λ = 1.996 X + 0.023

$$X = \frac{\Delta_{td,m}}{(2\,\Delta_t - \Delta_{td,m})}$$

Where, $\Delta_{td,m}$ = maximum inter-storey drift ratio (MIDR) for the building

Δ_t = target MIDR **[2]**

CHAPTER 6

BLAST RESISTANT DESIGN OF RC FRAMES

Analysis is carried out on a planar six-storey RC frame structure and a nine-storey RC frame structure to resist blast loading from distant blast explosions. The frame structure is shown in Fig. 6.1. The blast loads considered are 80t TNT at 100 m and 30t TNT at 100m for 6-storey and 30t TNT at 100 m for 9-storey. Since the blast waves are distant, the hemispherical surface blast wave produced at 100 m is modelled as a planar wave on the front of the building.

The basic design objective is to ensure that the MIDR of the RC designed frame structure is within the target MIDR, so that the performance level is within expectation.

The flowchart below in Fig. 6.2 shows how to design a RC frame subjected to blast loading based on ESF. The procedure mentioned is iterative.

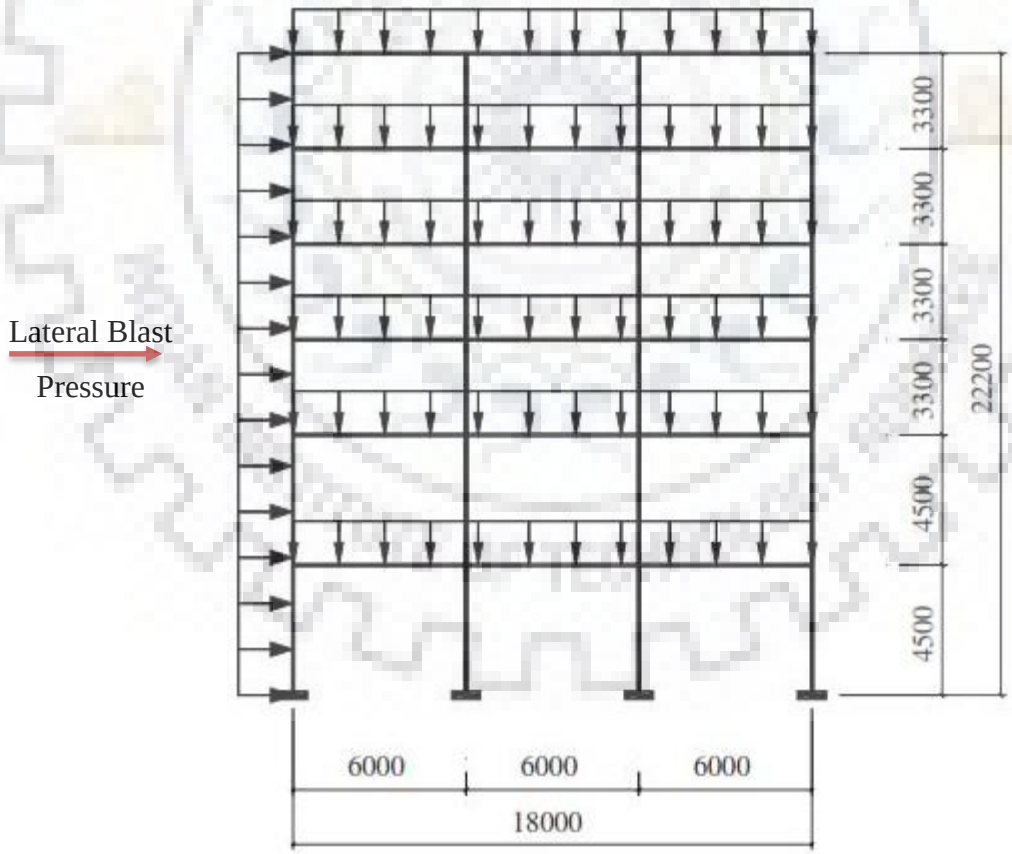

Fig. 6.1: RC frame having a uniform lateral blast pressure and a DL acting vertically = 30 KN/m

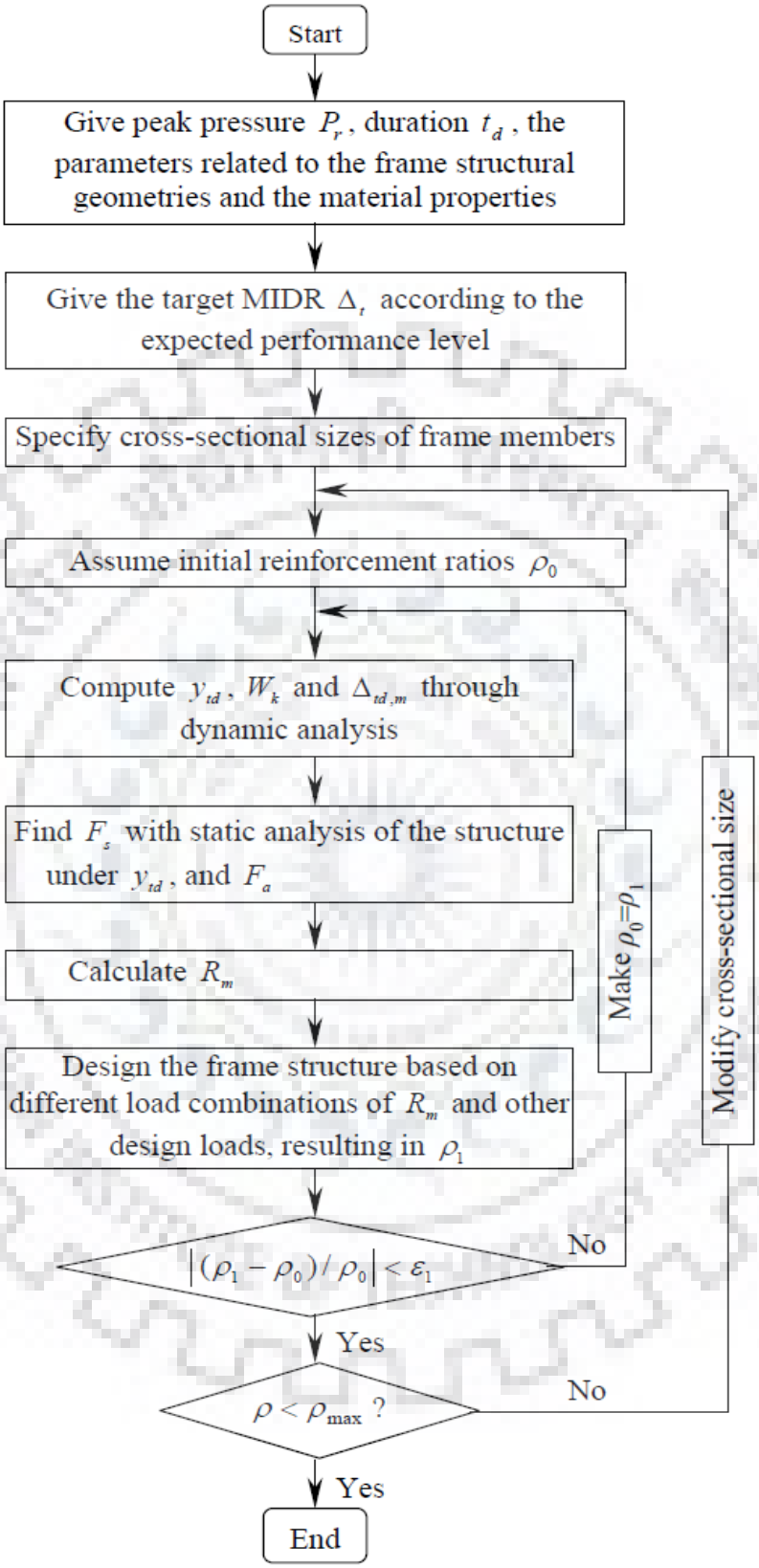

Figure 6.2 Flowchart of blast resistant design of a multi-storey reinforced concrete frame structure with ESF (e_1 is an arbitrarily small value)

Table 6.1: Frame member sections (6-storey)

Storey Level	Height (mm)	Width (mm)	Column Section (mm x mm)	Beam Section (mm x mm)
1-2	4500	3 x 6000	600 x 600	300 x 600
3-6	3300	3 x 6000	500 x 500	300 x 600

For the 9-storey building similar 500 mm x 500 mm columns and 300 mm x 600 mm beams are added above the 6 storey frame.

The member section is shown in Table 6.1 and its cross-sectional details of the beams and columns used in frame is shown in Fig. 6.3.

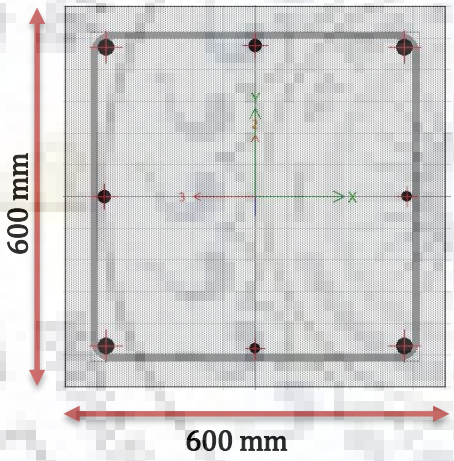

Fig. 6.3. a) Sectional detail of Column @ Storey 1,2

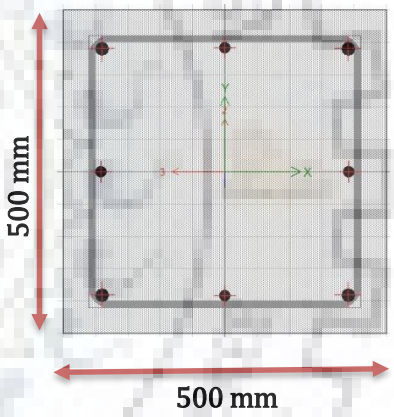

b) Sectional detail of Column @ Storey 3,4,5,6

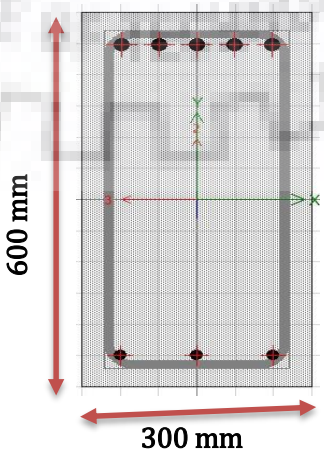

Fig. 6.3. c) Sectional detail of Beam

6.1 BLAST ANALYSIS AND DESIGN OF A 6-STOREY RC FRAME FOR 80 tonne TNT SURFACE BLAST AT 100m STANDOFF DISTANCE

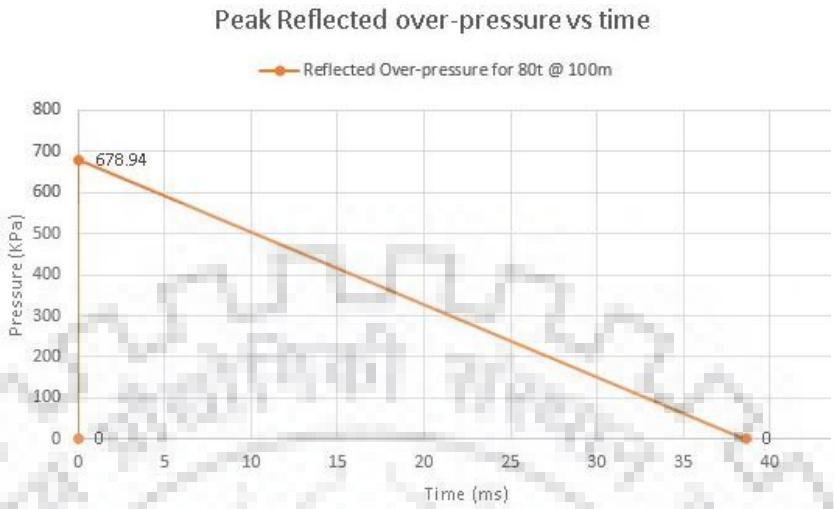

Fig 6.4.: Lateral blast pressure vs time for 80t TNT @ 100m

The hemispherical blast wave at 100 m was reasonably modelled as a planar wave on the front face of the building. The peak reflected over-pressure of 678.94 KPa as a triangular variation for a time of 38.6 milliseconds was applied. Here, the vertical roof pressures and the rear pressure was ignored as carried out in previous research paper **[7]**. The loading profile on the frame included superimposed Dead load = 30 KN/m along with the blast load.

In this design, a low performance level was given to the frame structure, for which an MIDR target of Δ_t = 3.5% was assigned, which is slightly less than the MIDR limit of 4% corresponding to which structure may lose its integrity or even collapse. **[2]**.

At the start of the design, cross-sectional sizes for frame members were assigned as 600 mm x 600 mm for first and second storey columns, 500 mm x 500 mm for remaining columns and 300 mm x 600 mm for all the beam members. Initial reinforcement ratios given were 0.8% longitudinal reinforcement for columns and for beams (0.8% /0.3%) for end span and (0.3%/0.6%) for mid span. $P_{st,i}$, which is the equivalent static point force vector was calculated at each iterative step and applied on the frame along with the DL = 30KN/m to design the reinforcement by ETABS.

Loading combinations used to design were of three types: (1.4 DL + 1.0 $P_{st,i}$, 1.4DL – 1.0 $P_{st,i}$, 1.4DL). The convergence criteria for reinforcement was defined as

$$\frac{|\rho_1 - \rho_0|}{\rho_0} \leq 0.05$$

Design Procedure

The First Iterative Design Step:

Storey (I)	$y_{td,i}$ (mm)	velocity (m/sec)	$W_{k,i}$ (KN m)	$F_{a,i}$ (KN)	$F_{s,i}$ (KN)	P_i (KN)	Δ	X	λ	$P_{st,,i}$ (KN)
6	10.787	0.479	7.666	1421.281	-634.447	786.834	0.663	0.105	0.232	182.274
5	19.996	0.682	16.518	1652.167	720.368	2372.535				549.609
4	20.367	0.783	21.768	2137.550	148.943	2286.493				529.677
3	20.623	0.864	26.549	2574.704	-964.097	1610.607				373.105
2	28.410	1.101	45.419	3197.413	474.809	3672.222				850.688
1	29.813	0.906	32.464	2177.820	1096.343	3274.163				758.476

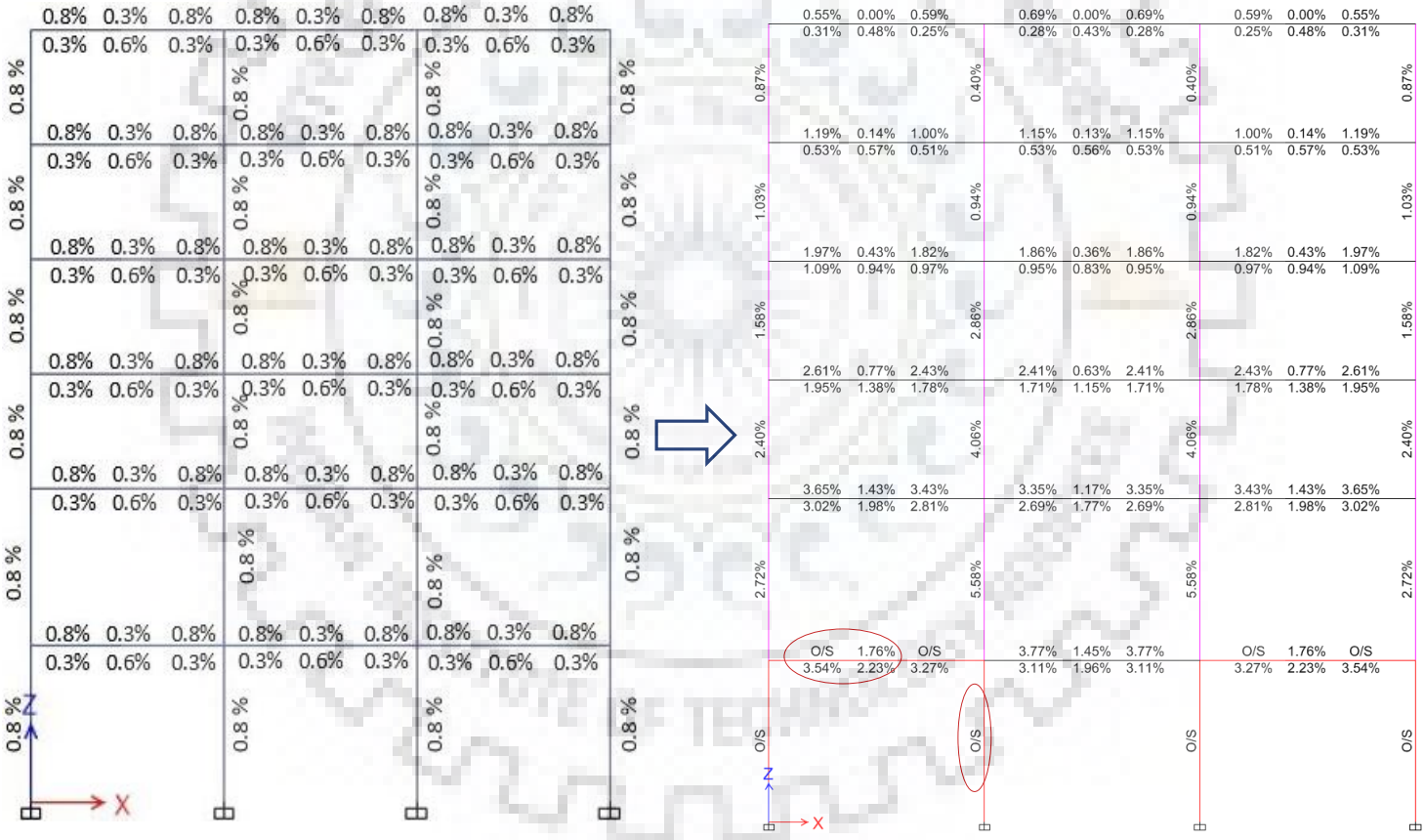

a) Initial Reinforcement Ratios (%) b) New Reinforcement Ratios (%)

Observation: After the 1st iteration, some frame members (Storey-1 columns and a few beams) are found to be over-stressed (that is, reinforcement found in these members are more than the maximum reinforcement allowed by the civil design code) represented as O/S. The Indian Standard civil code IS 456 allows for the maximum reinforcement to be provided as 6% for columns and 4% each for compression and tension reinforcement in beam..

These reinforcement are substituted as the new reinforcement ratios in over-stressed members and analyzed again for blast loads.

The Second Iterative Design Step:

Storey (I)	$y_{td,\,i}$ (mm)	velocity (m/sec)	$W_{k,i}$ (KN m)	$F_{a,i}$ (KN)	$F_{s,i}$ (KN)	P_i (KN)	Δ	X	λ	$P_{st,i}$ (KN)
6	10.747	0.479	7.659	1425.379	-565.689	859.690	0.622	0.097	0.218	187.028
5	20.113	0.688	16.818	1672.320	717.910	2390.230				520.000
4	20.339	0.786	21.923	2155.779	50.890	2206.669				480.066
3	20.877	0.878	27.372	2622.245	-1108.050	1514.195				329.417
2	28.427	1.110	46.161	3247.677	-29.450	3218.227				700.133
1	27.976	0.718	20.384	1457.251	5104.150	6561.401				1427.448

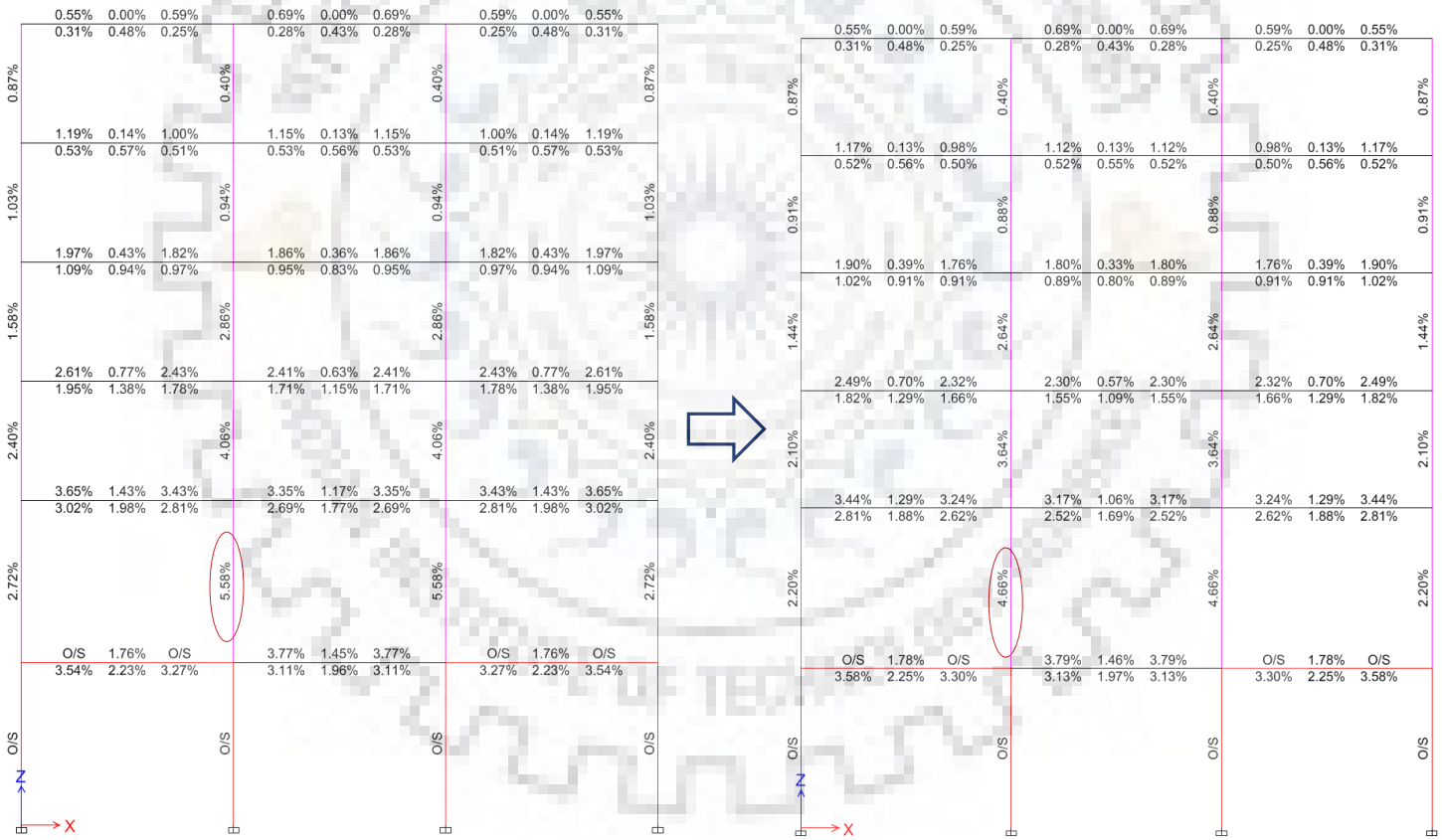

a) Initial Reinforcement Ratios (%) b) New Reinforcement Ratios (%)

Observation: After the second iteration, frame members still remain overstressed, though the reinforcement ratios in most members have reduced. So, before the third iteration is performed, the cross-sectional size of columns at Storey-1 is modified to 700mm X 700mm.

Table 6.2: Frame structure modified size

Storey Level	Height (mm)	Width (mm)	Column Section (mm x mm)	Beam Section (mm x mm)
1	4500	3 x 6000	700 x 700	300 x 600
2	4500	3 x 6000	600 x 600	300 x 600
3-6	3300	3 x 6000	500 x 500	300 x 600

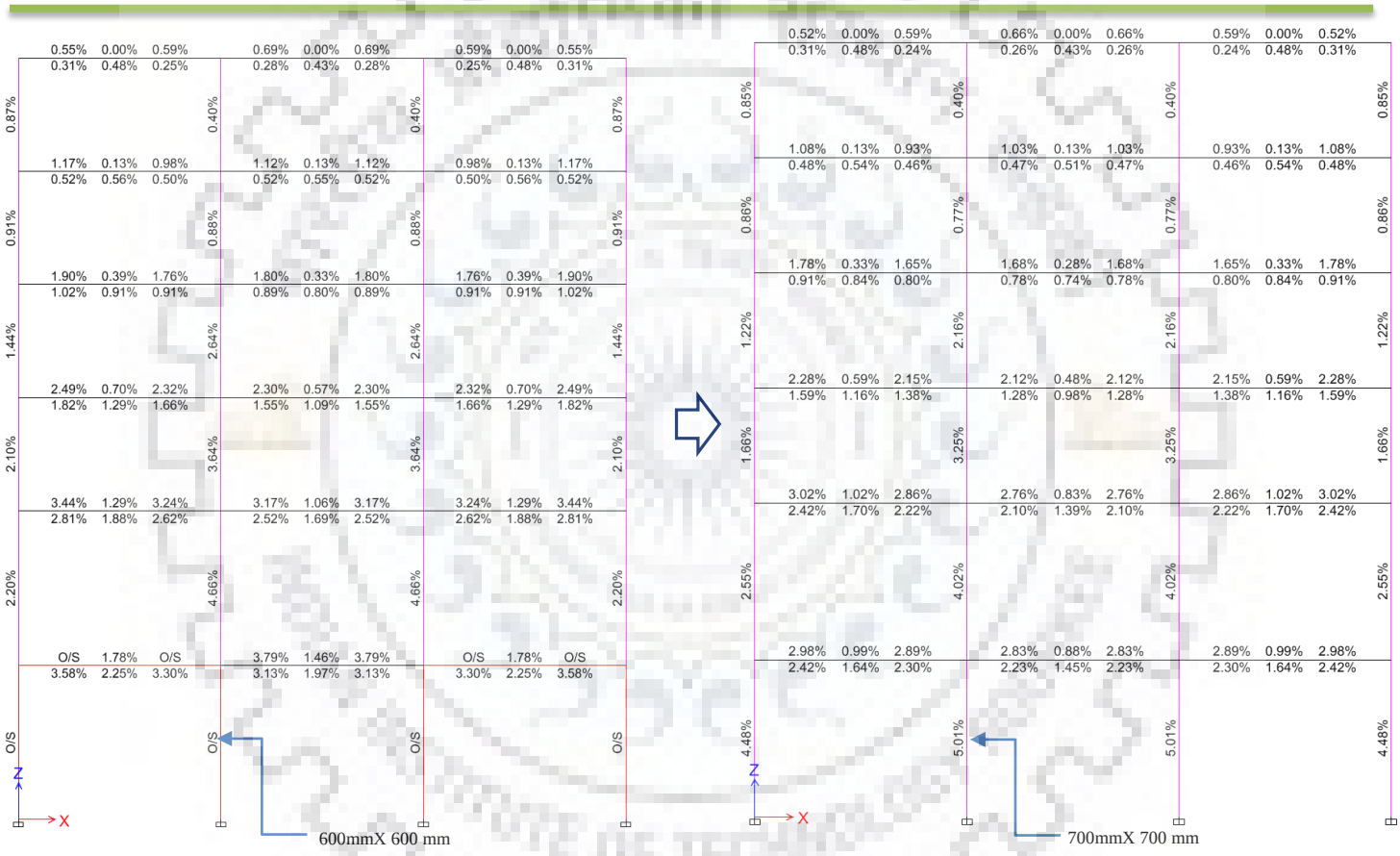

a) Initial Reinforcement Ratios (%)

b) New Reinforcement Ratios (%)

The Third Iterative Design Step:

Storey (I)	$y_{td,i}$ (mm)	velocity (m/sec)	$W_{k,i}$ (KN m)	$F_{a,i}$ (KN)	$F_{s,i}$ (KN)	P_i (KN)	Δ	X	λ	$P_{st,i}$ (KN)
6	10.727	0.479	7.668	1429.589	-564.730	864.859	0.511	0.079	0.180	155.832
5	20.088	0.689	16.849	1677.518	717.470	2394.988				431.534
4	20.299	0.785	21.879	2155.630	63.860	2219.490				399.913
3	20.920	0.891	28.188	2694.884	-1287.110	1407.774				253.656
2	28.559	1.105	45.747	3203.659	440.040	3643.699				656.530
1	22.995	0.393	6.117	532.030	6393.820	6925.850				1247.916

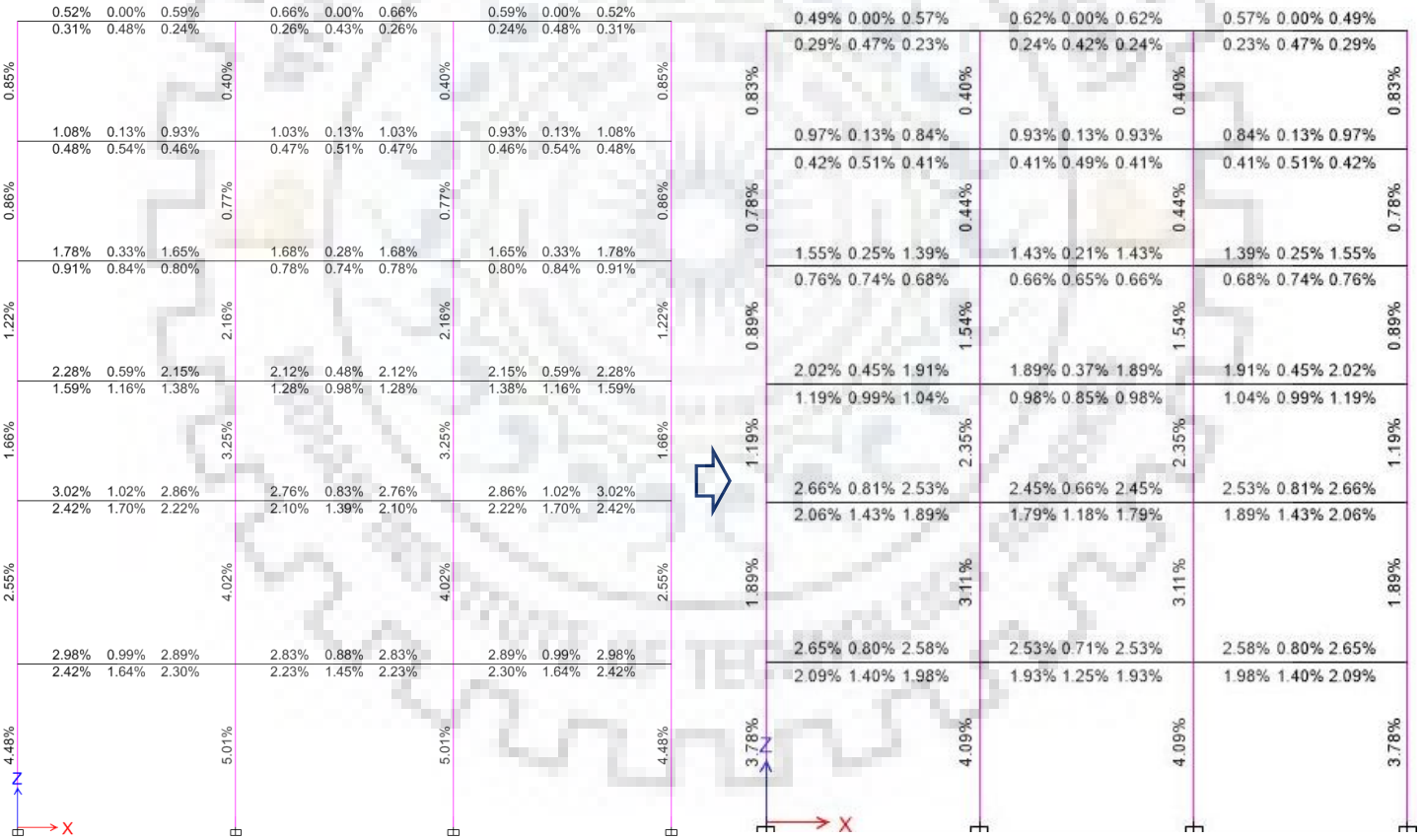

a) Initial Reinforcement Ratios (%)

b) New Reinforcement Ratios (%)

The Fourth Iterative Design Step:

Storey (I)	$y_{td,\,i}$ (mm)	velocity (m/sec)	$W_{k,i}$ (KN m)	$F_{a,i}$ (KN)	$F_{s,i}$ (KN)	P_i (KN)	Δ	X	λ	$P_{st,i}$ (KN)
6	10.759	0.479	7.655	1423.076	-513.63	909.45	0.510	0.079	0.180	163.701
5	20.118	0.689	16.880	1678.083	607.93	2286.02				411.484
4	20.395	0.788	22.050	2162.249	143.01	2305.26				414.947
3	20.957	0.891	28.223	2693.389	-1374.50	1318.89				237.400
2	28.635	1.103	45.622	3186.427	626.45	3812.88				686.319
1	22.933	0.401	6.340	552.951	5267.04	5819.99				1047.599

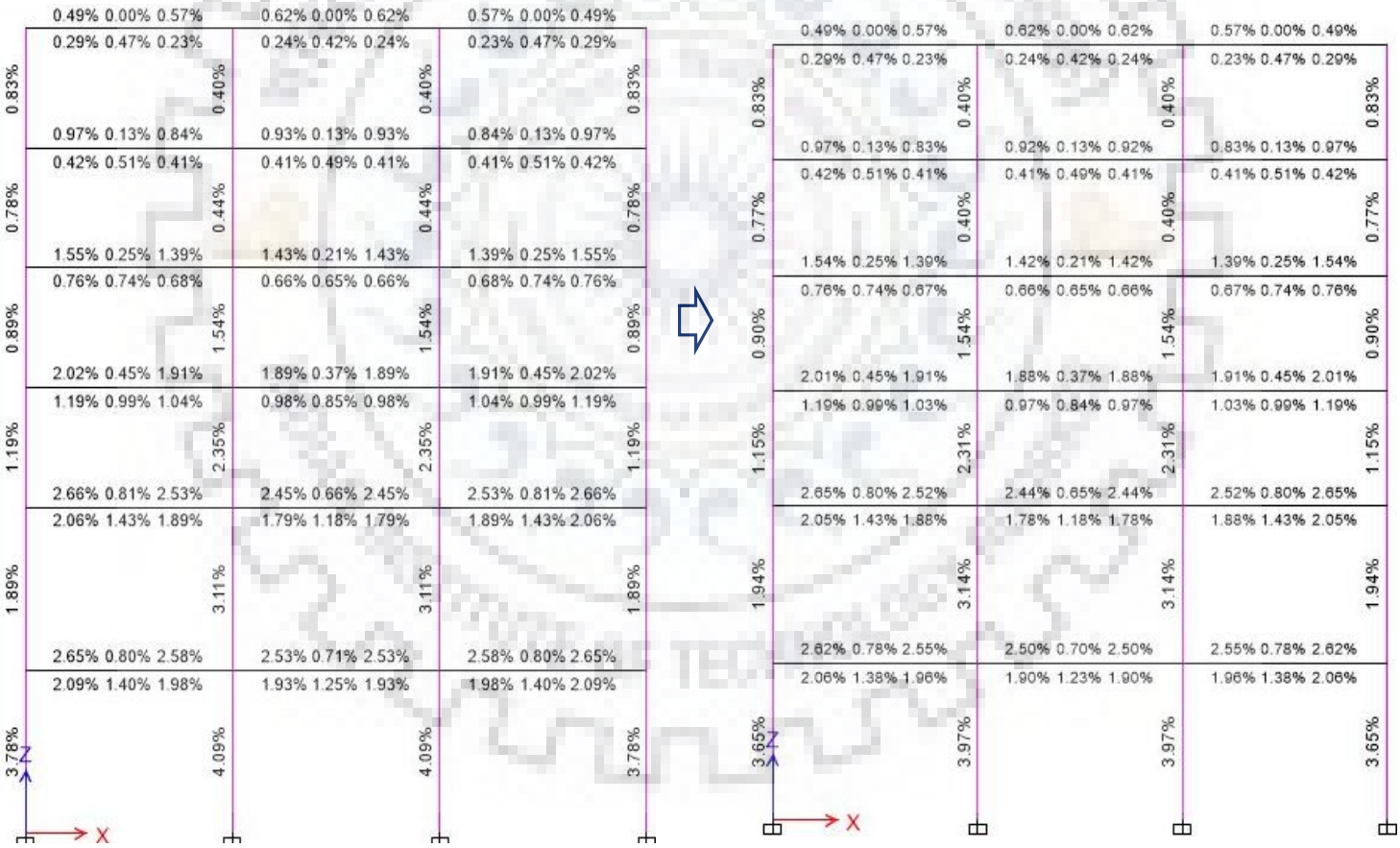

a) Initial Reinforcement Ratios (%)

b) New Reinforcement Ratios (%)
[FINAL DESIGN]

6.1.1. Response of the Designed Frame Structure under the given blast force

The final designed RC frame was now subjected to the blast load and analyzed for a longer time, much after the blast load had stopped acting on the structure. As expected, the MIDR occurred at a time later than the blast loading duration t_d.

Table 6.3: MIDR at various storey levels (80t TNT)

STOREY LEVEL	MIDR (%)
6	0.99
5	1.21
4	1.17
3	1.23
2	1.04
1	0.55

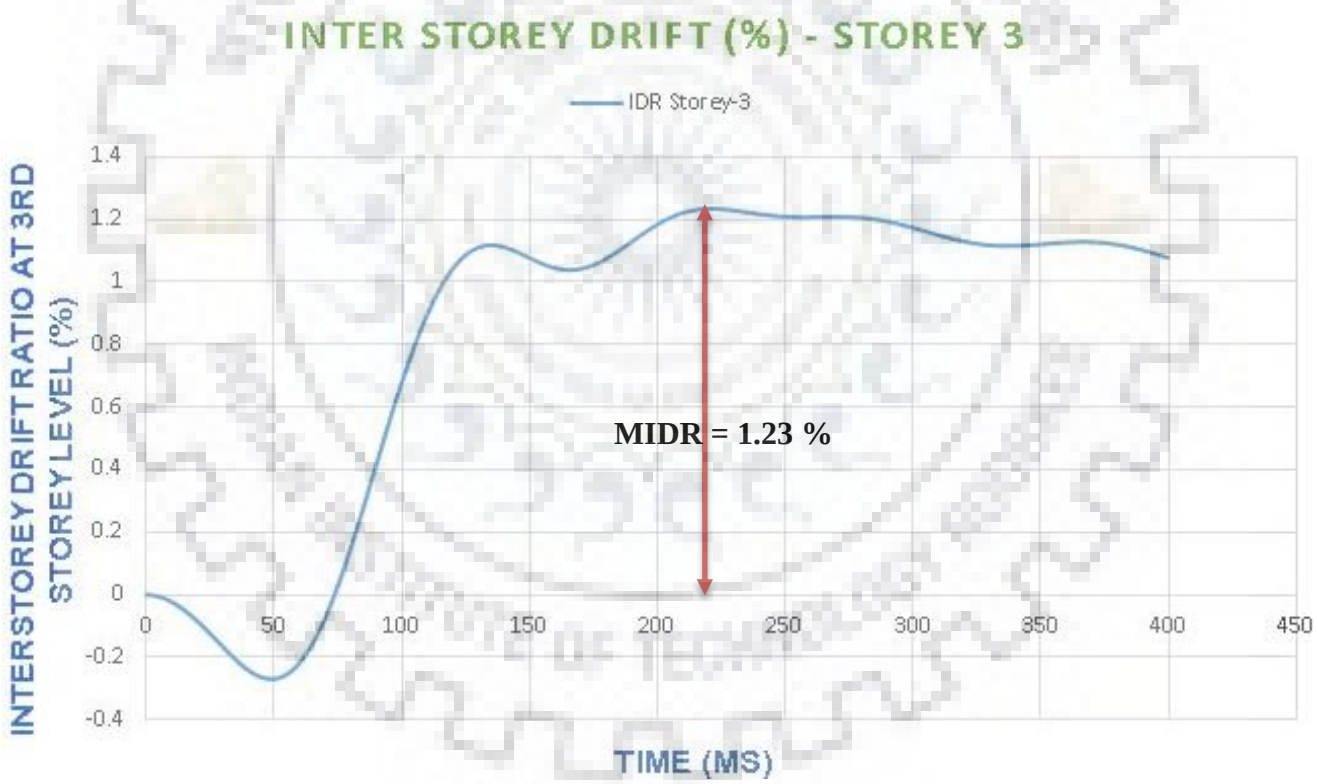

Fig 6.5.: Graph showing MIDR = 1.23% (80t TNT)

6.1.2. Conclusion

The MIDR at the critical story (3rd Story) was found to be 1.23% which was well below the target MIDR of 3.5% allowed in the building. Since, the cross-sectional sizes provided initially were not sufficient as the reinforcement ratios had exceeded the maximum allowed longitudinal reinforcement ratio, the cross-sectional size of the column at Storey-1 was accordingly modified to be 700mm x 700 mm.

6.2. BLAST ANALYSIS AND DESIGN OF A 6-STOREY RC FRAME FOR 30 tonne TNT SURFACE BLAST AT 100m STANDOFF DISTANCE

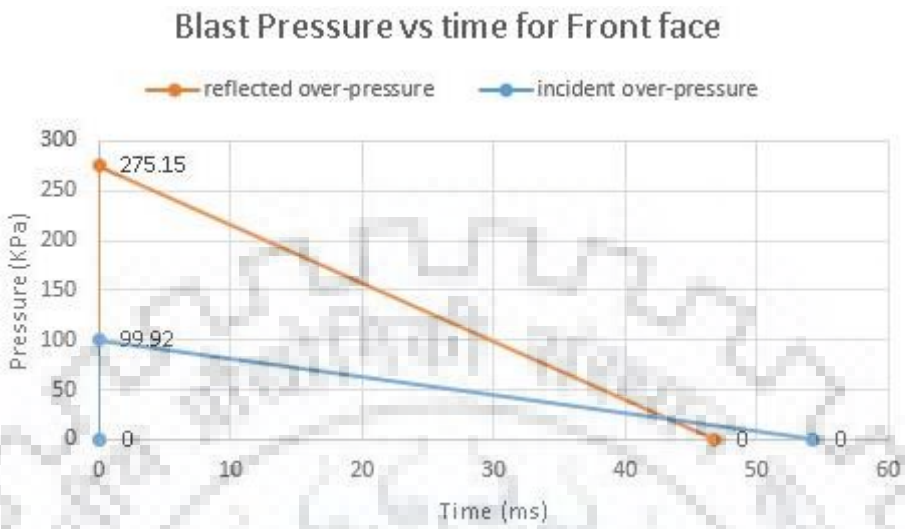

Fig 6.6.: Blast pressure vs time for front face (Clearance time = 58.3 ms > t_{of} = 54.23 ms)

The peak reflected over-pressure of 275.15 KPa as a triangular variation for a time of 46.7 milliseconds was applied. As, for the previous case of 80t TNT blast, all the loading conditions were kept similar. Here also, the vertical roof pressures and the rear pressure was ignored.**[7]**.

However, in this design, a high performance level was given to the frame structure, and thus a lower target MIDR of Δ_t = 1.5% was assigned. **[2]**

The cross-sectional sizes along with the loading combinations and reinforcement convergence criteria was also kept similar.

The First Iterative Design Step:

Storey (I)	$y_{td,i}$ (mm)	velocity (m/sec)	$W_{k,i}$ (KN m)	$F_{a,i}$ (KN)	$F_{s,i}$ (KN)	P_i (KN)	Δ	X	λ	$P_{st,i}$ (KN)
6	6.632	0.255	2.167	653.585	-527.499	126.086	0.355	0.134	0.291	36.710
5	11.370	0.302	3.248	571.319	589.447	1160.766				337.958
4	12.113	0.383	5.224	862.597	61.692	924.289				269.108
3	12.498	0.444	7.018	1123.116	-657.020	466.096				135.704
2	16.905	0.546	11.186	1323.451	382.381	1705.832				496.655
1	15.990	0.310	3.793	474.455	987.348	1461.804				425.605

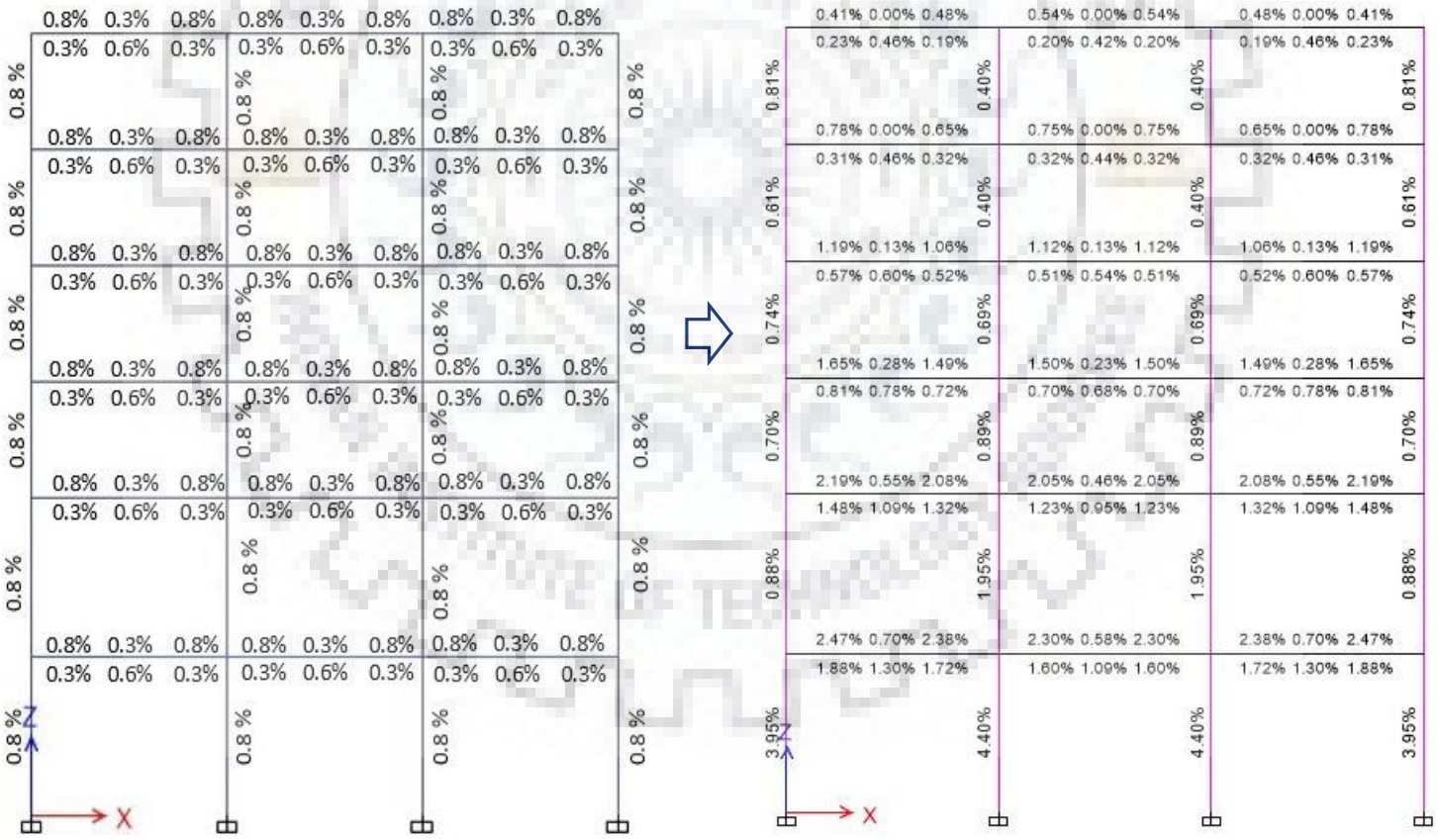

a) Initial Reinforcement Ratios (%)

b) New Reinforcement Ratios (%)

The Second Iterative Design Step:

Storey (I)	$y_{td,i}$ (mm)	velocity (m/sec)	$W_{k,i}$ (KN m)	$F_{a,i}$ (KN)	$F_{s,i}$ (KN)	P_i (KN)	Δ	X	λ	$P_{st,i}$ (KN)
6	6.521	0.248	2.062	632.377	-464.506	167.871	0.334	0.125	0.273	45.811
5	11.469	0.307	3.346	583.449	529.279	1112.728				303.656
4	12.110	0.387	5.324	879.314	25.125	904.439				246.815
3	12.707	0.455	7.347	1156.335	-632.834	523.501				142.860
2	16.803	0.531	10.553	1256.050	204.312	1460.362				398.523
1	15.022	0.254	2.549	339.317	2499.400	2838.717				774.666

a) Initial Reinforcement Ratios (%)

b) New Reinforcement Ratios (%)

The Third Iterative Design Step:

Storey (I)	$y_{td,i}$ (mm)	velocity (m/sec)	$W_{k,i}$ (KN m)	$F_{a,i}$ (KN)	$F_{s,i}$ (KN)	P_i (KN)	Δ	X	λ	$P_{st,i}$ (KN)
6	6.523	0.249	2.067	633.763	-458.894	174.869	0.333	0.125	0.272	47.588
5	11.500	0.308	3.363	584.914	531.142	1116.056				303.718
4	12.091	0.387	5.318	879.604	11.162	890.767				242.409
3	12.709	0.455	7.350	1156.611	-617.580	539.030				146.689
2	16.810	0.530	10.544	1254.439	221.328	1475.767				401.608
1	14.980	0.253	2.524	336.927	2405.077	2742.004				746.196

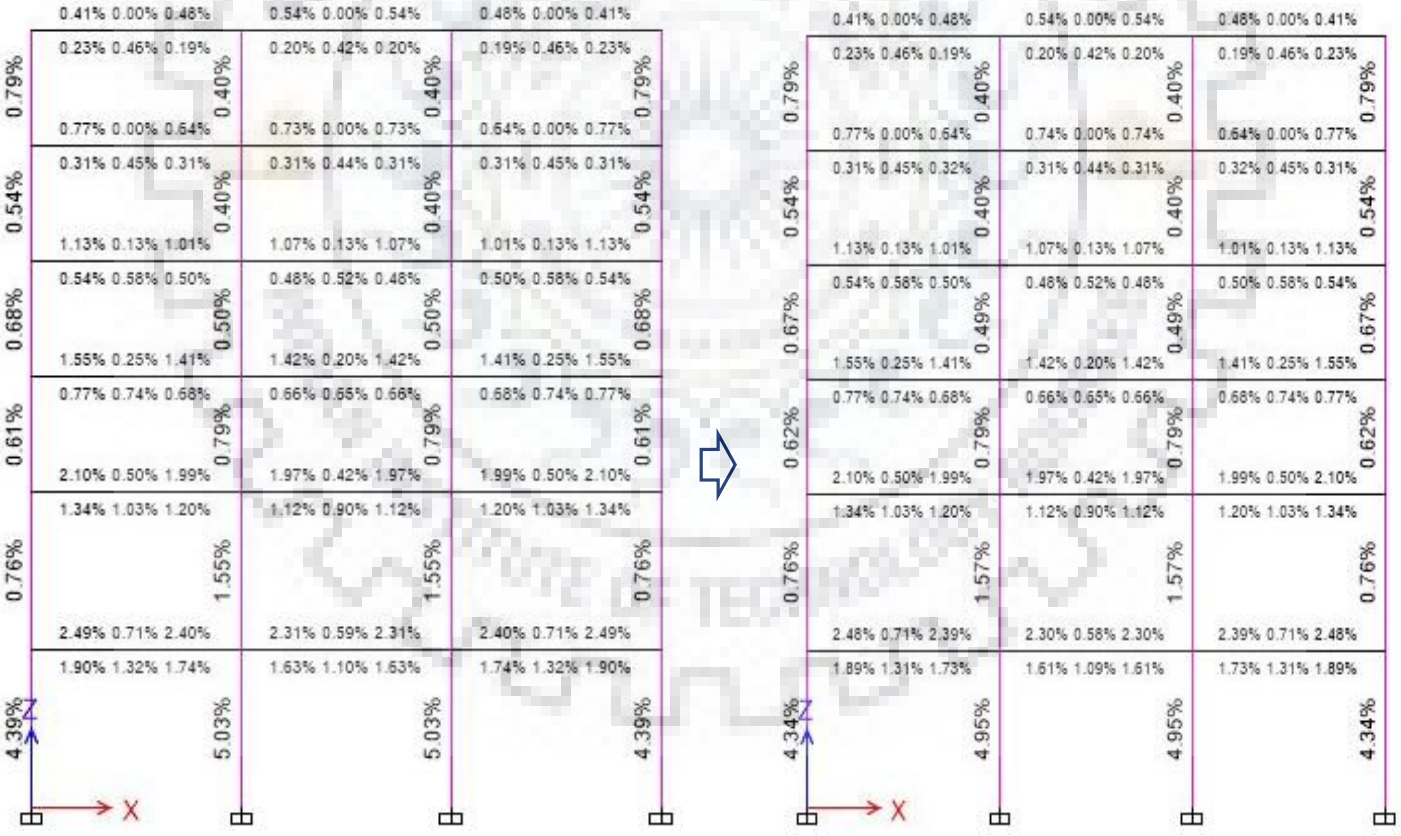

a) Initial Reinforcement Ratios (%)

b) New Reinforcement Ratios (%)
[FINAL DESIGN]

6.2.1. Responses of the Designed Frame Structure under the given blast force

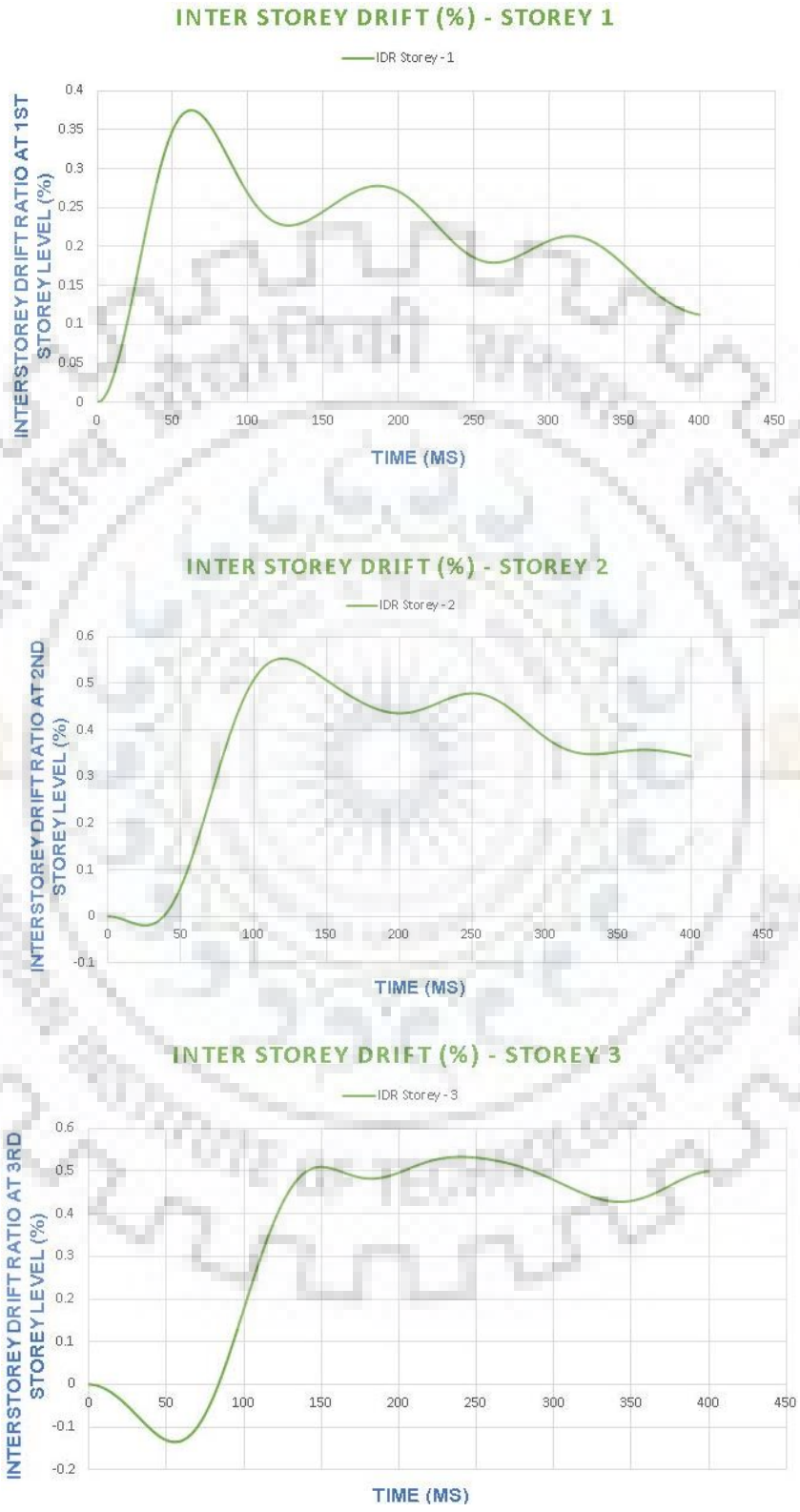

Fig 6.7 (a) : Interstorey Drift Ratio vs Time at 1st , 2nd , 3rd Storey Level

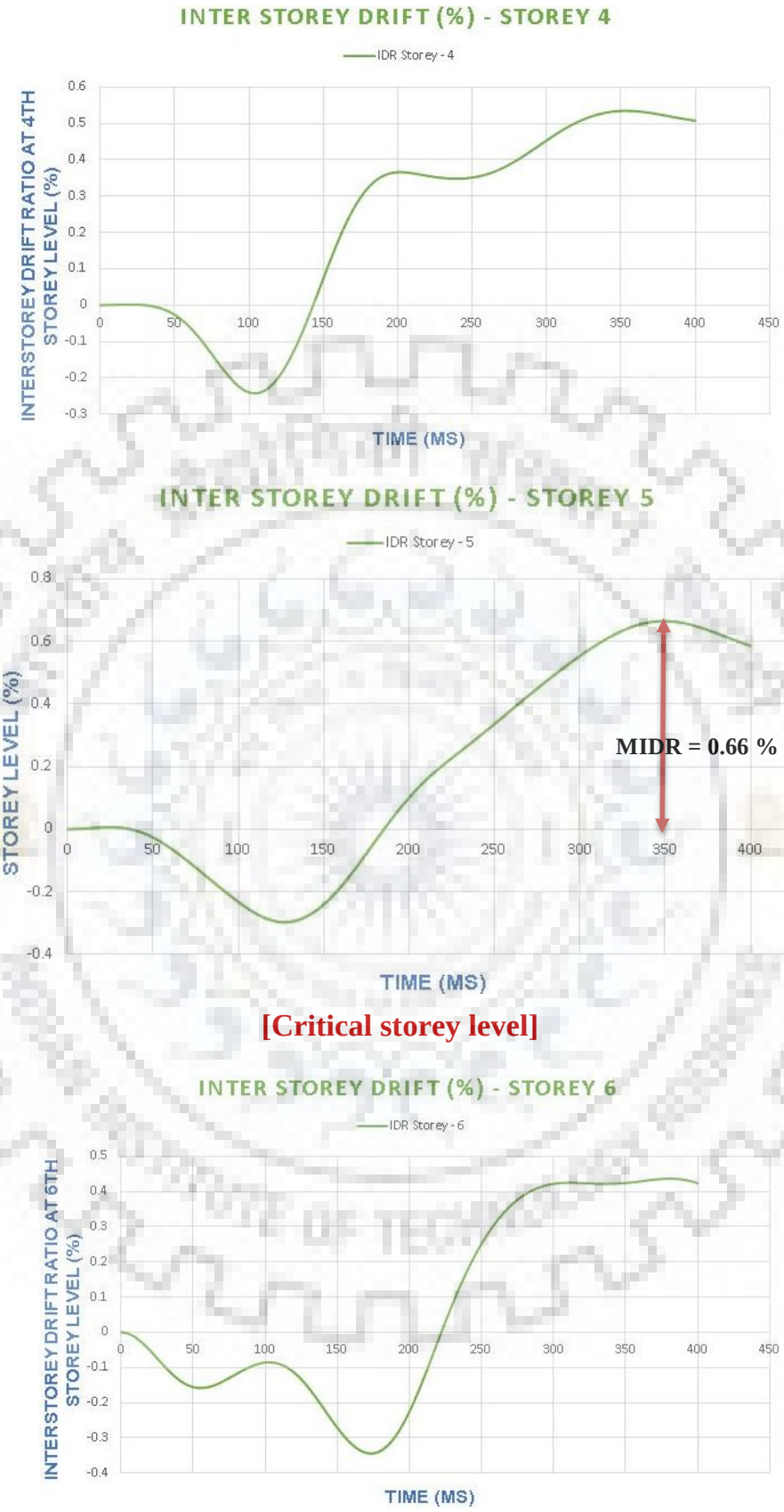

Fig 6.7 (b) : Interstorey Drift Ratio vs Time at 4th, 5th , 6th Storey Level

Table 6.4: IDR at various storey levels (30t TNT)

STOREY LEVEL	IDR (%)
6	0.44
5	0.66
4	0.53
3	0.53
2	0.55
1	0.38

6.2.2 Summary

It can be seen that the convergence with ESF was rapid as only three iterations were needed. The MIDR at the critical story (5rd Story) was found to be 0.66% which was well below the target MIDR of 1.5% allowed in the building. Moreover, the reinforcement ratios obtained were all within the maximum allowable longitudinal reinforcement ratio, thus the cross-sectional sizes of the members were kept as those initially specified.

6.3 BLAST ANALYSIS AND DESIGN OF A 9-STOREY RC FRAME FOR 30 tonne TNT SURFACE BLAST AT 100m STANDOFF DISTANCE

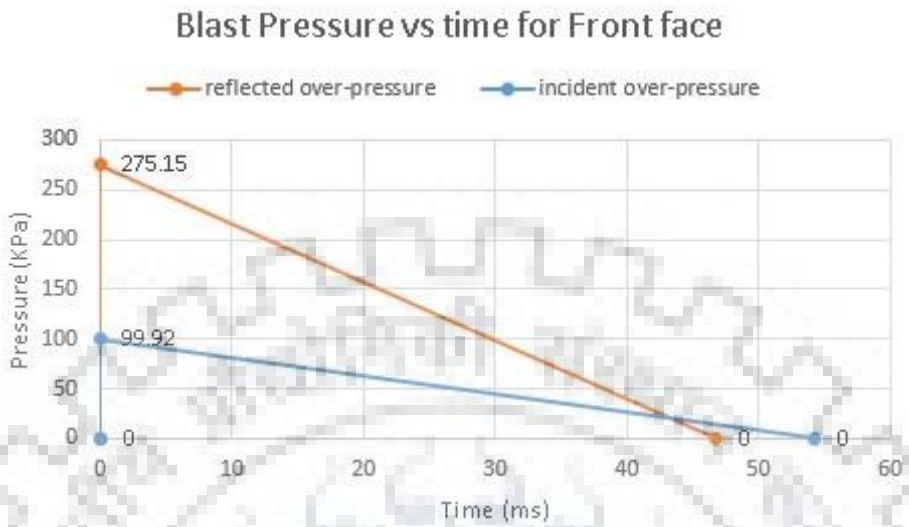

Fig 6.8.: Blast pressure vs time for front face (Clearance time = 58.3 ms > t_{of} = 54.23 ms)

Along the similar lines of analysis and design of the frame structures as carried out for 6-storey frame, the hemispherical blast wave at 100 m was reasonably modelled as a planar wave on the front face of the building. The peak reflected over-pressure of 275.15 KPa as a triangular variation for a time of 46.7 milliseconds was applied. Here, the vertical roof pressures and the rear pressure was ignored as carried out in previous research paper **[7]**. The loading profile on the frame included superimposed Dead load = 30 KN/m along with the blast load.

In this design, MIDR target of Δ_t = 1.5% was assigned, which is less than the MIDR limit of 4% corresponding to which structure may lose its integrity or even collapse. **[2]**.

At the start of the design, cross-sectional sizes for frame members were assigned as 600 mm x 600 mm for first and second storey columns, 500 mm x 500 mm for remaining columns and 300 mm x 600 mm for all the beam members. Initial reinforcement ratios given were 0.8% longitudinal reinforcement for columns and for beams (0.8% /0.3%) for end span and (0.3%/0.6%) for mid span. $P_{st,i}$, which is the equivalent static point force vector was calculated at each iterative step and applied on the frame along with the DL = 30KN/m to design the reinforcement by ETABS.

Loading combinations used to design were of three types: (1.4 DL + 1.0 $P_{st,i}$, 1.4DL – 1.0 $P_{st,i}$, 1.4DL). The convergence criteria for reinforcement was defined as

$$\frac{|\rho_1 - \rho_0|}{\rho_0} \leq 0.05$$

The First Iterative Design Step:

Storey (I)	$y_{td,i}$ (mm)	velocity (m/sec)	$W_{k,i}$ (KN m)	$F_{a,i}$ (KN)	$F_{s,i}$ (KN)	P_i (KN)	Δ	X	λ	$P_{st,,i}$ (KN)
9	6.560	0.252	3.52	1072.36	-524.40	547.96				159.12
8	11.380	0.303	5.29	930.01	548.20	1478.21				429.24
7	12.403	0.401	9.27	1494.70	56.30	1551.00				450.38
6	11.995	0.383	8.44	1407.44	-112.80	1294.64				375.94
5	12.033	0.376	8.14	1353.26	75.10	1428.36	0.354	0.134	0.230	414.77
4	11.770	0.363	7.59	1289.52	26.40	1315.92				382.12
3	12.480	0.441	11.20	1795.36	-570.60	1224.76				355.65
2	16.930	0.548	17.90	2114.70	356.30	2471.00				717.53
1	15.950	0.304	5.70	714.77	988.90	1703.67				494.71

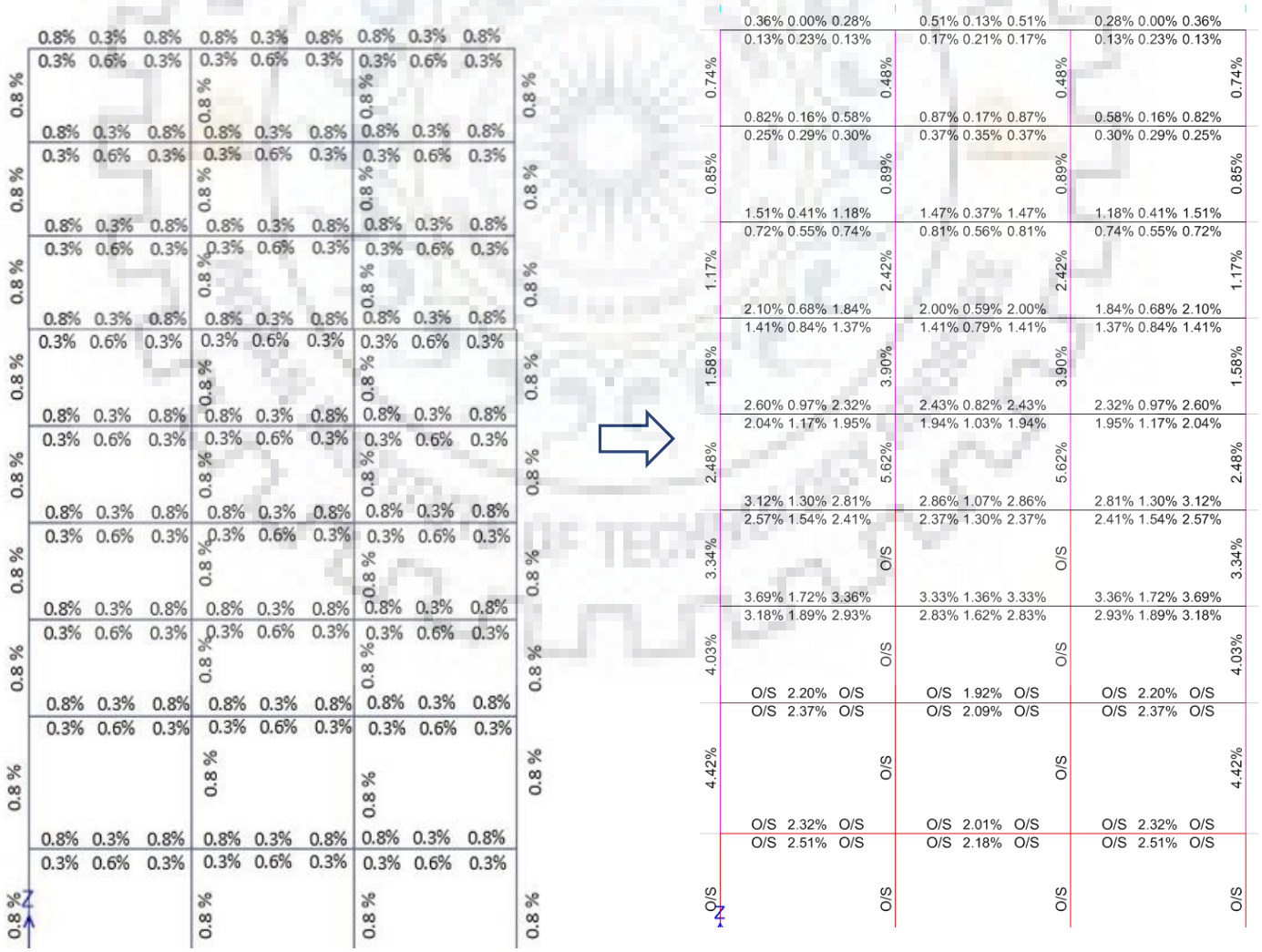

a) Initial Reinforcement Ratios (%)

b) New Reinforcement Ratios (%)

Observation: After the 1st iteration, some frame members (Columns od storeys 1,2,3,4 and a few beams) are found to be over-stressed (that is, reinforcement found in these members are more than the maximum reinforcement allowed by the civil design code) represented as O/S. The IS CODE IS 456 allows for the maximum reinforcement to be provided as 6% for columns and 4% each for compression and tension reinforcement in beam..

These reinforcement are substituted as the new reinforcement ratios in over-stressed members and analyzed again for blast loads.

The Second Iterative Design Step:

Storey (I)	$y_{td,i}$ (mm)	velocity (m/sec)	$W_{k,i}$ (KN m)	$F_{a,i}$ (KN)	$F_{s,i}$ (KN)	P_i (KN)	Δ	X	λ	$P_{st,i}$ (KN)
9	6.545	0.252	3.53	1077.38	-478.50	598.88	0.342	0.129	0.279	167.58
8	11.384	0.302	5.26	924.42	490.60	1415.02				395.95
7	12.38	0.401	9.24	1493.53	66.50	1560.03				436.53
6	12.015	0.383	8.45	1406.50	-106.40	1300.10				363.79
5	12.040	0.377	8.18	1358.02	69.70	1427.72				399.51
4	11.786	0.364	7.61	1291.89	-81.60	1210.29				338.66
3	12.486	0.446	11.44	1832.93	-624.70	1208.23				338.09
2	16.846	0.534	16.96	2013.30	177.90	2191.20				613.15
1	15.389	0.264	4.29	557.26	2561.80	3119.06				872.78

a) Initial Reinforcement Ratios (%) b) New Reinforcement Ratios (%)

Observation: After the second iteration, frame members still remain overstressed, though the reinforcement ratios in most members have reduced. So, before the third iteration is performed, the cross-sectional size of columns and beams are modified to make it less than the maximum limit prescribed.

Table 6.5: Frame structure modified size

Storey Level	Height (mm)	Width (mm)	Column Section (mm x mm)	Beam Section (mm x mm)
1 - 2	4500	3 x 6000	800 X 800	400 X 600
3 - 4	3300	3 x 6000	600 X 600	300 X 600
4 - 9	3300	3 x 6000	500 X 500	300 X 600

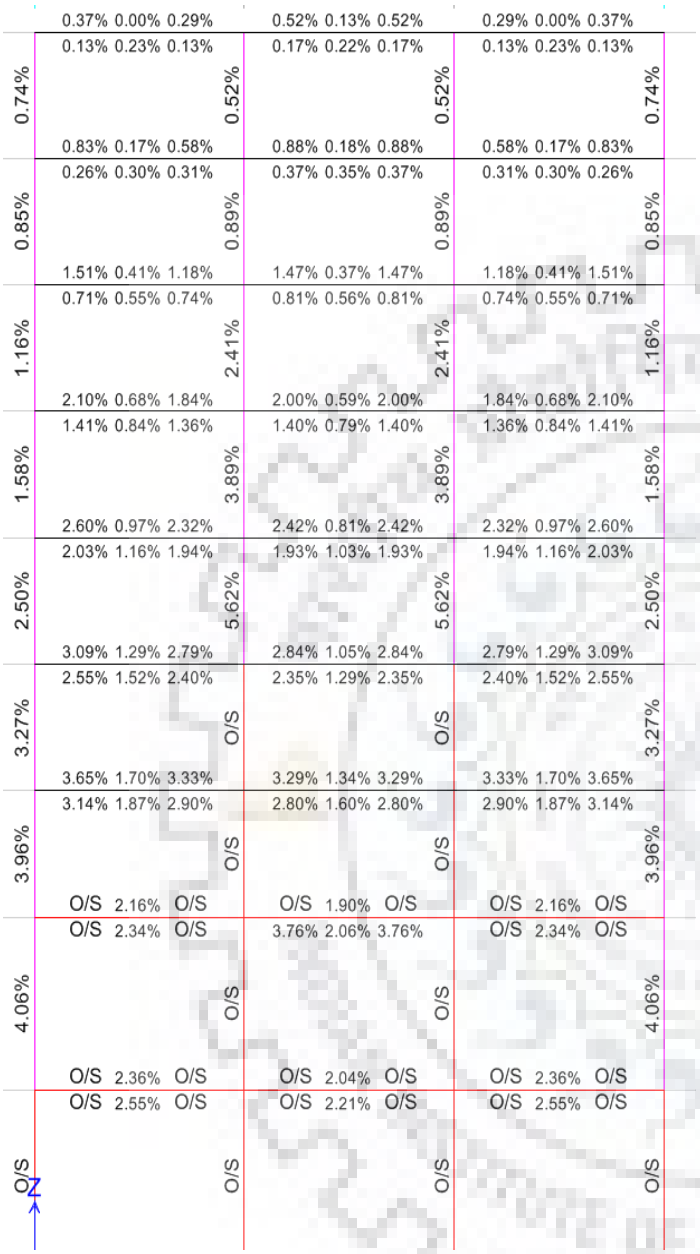

a) Initial Reinforcement Ratios (%)

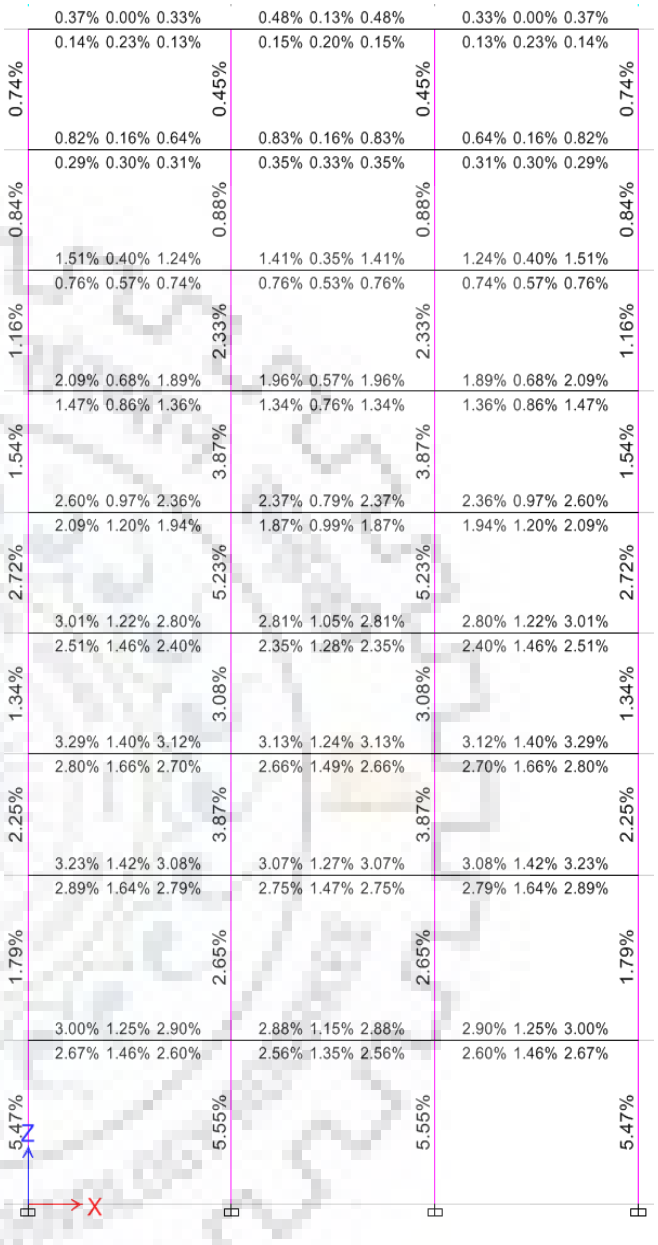

b) New Reinforcement Ratios (%)

The Third Iterative Design Step:

Storey (I)	$y_{td,i}$ (mm)	velocity (m/sec)	$W_{k,i}$ (KN m)	$F_{a,i}$ (KN)	$F_{s,i}$ (KN)	P_i (KN)	Δ	X	λ	$P_{st,i}$ (KN)
9	6.526	0.252	3.52	1079.06	-469.80	609.27	0.281	0.103	0.229	139.59
8	11.367	0.303	5.28	929.60	504.77	1434.37				328.64
7	12.346	0.402	9.30	1506.55	82.44	1588.98				364.07
6	12.068	0.392	8.84	1465.54	-111.14	1354.40				310.32
5	12.105	0.378	8.22	1358.55	97.42	1455.96				333.59
4	11.208	0.243	3.40	606.35	626.40	1232.75				282.45
3	11.874	0.337	6.54	1100.81	35.44	1136.25				260.33
2	13.831	0.358	7.63	1102.83	1406.61	2509.45				574.96
1	12.634	0.166	1.70	268.40	3061.80	3330.20				763.01

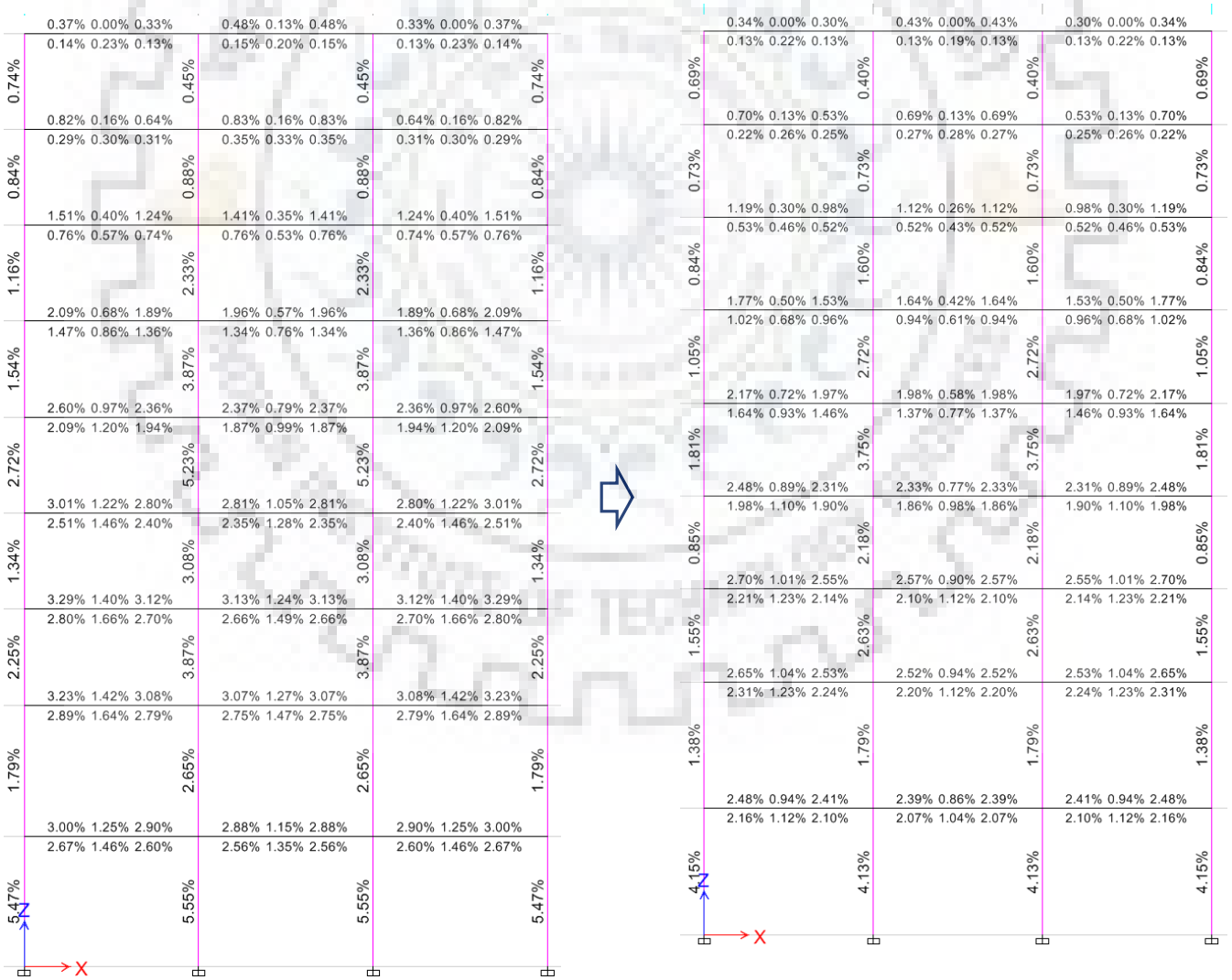

a) Initial Reinforcement Ratios (%)

b) New Reinforcement Ratios (%)

The Fourth Iterative Design Step:

Storey (I)	$y_{td,i}$ (mm)	velocity (m/sec)	$W_{k,i}$ (KN m)	$F_{a,i}$ (KN)	$F_{s,i}$ (KN)	P_i (KN)	Δ	X	λ	$P_{st,i}$ (KN)
9	6.515	0.252	3.521	1080.867	-442.414	638.453	0.282	0.104	0.230	146.64
8	11.313	0.302	5.249	927.853	436.497	1364.350				313.37
7	12.305	0.404	9.393	1526.673	117.977	1644.649				377.75
6	12.032	0.393	8.888	1477.436	-212.850	1264.586				290.46
5	12.087	0.377	8.179	1353.390	177.407	1530.796				351.60
4	11.155	0.244	3.426	614.254	557.659	1171.913				269.17
3	11.853	0.377	8.179	1380.079	-221.704	1158.376				266.06
2	13.794	0.361	7.755	1124.385	1411.476	2535.861				582.45
1	12.668	0.172	1.820	287.381	2886.440	3173.821				728.98

a) Initial Reinforcement Ratios (%)

b) New Reinforcement Ratios (%) **[FINAL DESIGN]**

6.3.1. Response of the Designed Frame Structure under the given blast force

The final designed RC frame was now subjected to the blast load and analyzed for a longer time, much after the blast load had stopped acting on the structure. As expected, the MIDR occurred later than the blast loading duration t_d.

Table 6.6: IDR at various storey levels for a 9-storey (30t TNT)

STOREY LEVEL	IDR (%)
9	0.46
8	0.56
7	0.59
6	0.62
5	0.61
4	0.57
3	0.54
2	0.47
1	0.32

Fig 6.9.: Graph showing MIDR = 0.62% for 9-storey RC frame (30t TNT)

6.3.2. Conclusion

The MIDR at the critical story (6th Story) was found to be 0.623% which was well below the target MIDR of 1.5% allowed in the building. Since, the cross-sectional sizes provided initially were not sufficient as the reinforcement ratios had exceeded the maximum allowed longitudinal reinforcement ratio, the cross-sectional size of the column and beams were modified as given in Table 6.6.

CHAPTER 7

CONCLUSION

7.1 SUMMARY

In this work, the analysis and design of reinforced concrete frames under distant blast was carried out. To meet the expected global performance level of a multi-storey RC frame under the distant explosion conditions, its MIDR response was kept under proper control after being loaded with the ESF.

An equivalent static system is constructed for the purpose of simulating the kinetic energy at t_d by the strain energy of the additional springs. According to the equilibrium of the equivalent static system, the external static force is obtained, however this force will produce a larger MIDR demand than that of the frame structure under the blast condition and thus the ESF factor λ is introduced to reduce the external static force to finally obtain the ESF. By comparing the nonlinear dynamic responses of frame structures with corresponding nonlinear static pushover analytical results, the value of is obtained as an empirical equation.

This ESF is applied to the frame structure and the goal is to ensure MIDR responses with the required design target into the design of a multi-storey reinforced concrete frame structure. For given cross- sectional sizes of the frame members, the reinforcement ratios are iteratively solved. The iteration procedure is shown in a flow chart. Three numerical examples varying both in TNT charge weight and storey height shows that there is no difficulty in getting computational convergence for the design method based on ESF.

7.2 CONCLUSION

The conclusion of the ESF based MIDR response for a 6-storey RC frame subjected to 80t TNT at 100 m and 30t TNT at 100 m along with the MIDR response of the 30t TNT at 100 m for a 9-storey building shows that the procedure provided to design the building for the blast resistance is working and can be used. A summary of the conclusions is shown below.

1. Taking the MIDR response parameter as the global performance indicator, a performance-based blast resistant design approach is presented for the multi- storey reinforced concrete frame structural system by using the equivalent static force (ESF). This approach is firstly addressed for the design of a SDOF system controlling its maximum displacement response and then extended into the design of a frame structure controlling its MIDR response.

2. By replacing the ESF with the ultimate strength and the maximum displacement/MIDR response with the required design target, the calculation model of the ESF is implemented into the design of an elastic-perfectly- plastic multi-storey reinforced concrete frame structural system. The ultimate strength for the SDOF system/the reinforcement ratios of the frame members for the given cross-sectional sizes can be iteratively solved during the design in order to satisfy the target displacement/MIDR.

3. The presented performance-based design procedures using ESF have been illustrated, which display that there is no difficulty in convergence of the iterative procedures.

4. The MIDR at the critical story (3^{rd} Story) for a 6-storey RC frame with 80t TNT at 100 m was found to be 1.23% which was well below the target MIDR of 3.5% allowed in the building. Since, the cross-sectional sizes provided initially were not sufficient as the reinforcement ratios had exceeded the maximum allowed longitudinal reinforcement ratio, the cross-sectional size of the column at Storey-1 was accordingly modified to be 700mm x 700 mm.

5. It can be seen that for the similar 6-storey RC frame with 30t TNT at 100 m ,the MIDR at the critical story (5^{rd} Story) was found to be 0.66% which was well below the target MIDR of 1.5% allowed in the building. Moreover, the reinforcement ratios obtained were all within the maximum allowable longitudinal reinforcement ratio, thus the cross-sectional sizes of the members were kept as those initially specified.

6. When the 9-storey frame was acted upon by 30t TNT at 100 m, the MIDR at the critical story (6th Story) was found to be 0.62% which again was below the target MIDR of 1.5% allowed in the building. Since, the cross-sectional sizes provided initially were not sufficient as the reinforcement ratios had exceeded the maximum allowed longitudinal reinforcement ratio, the cross-sectional size of the column and beam were increased accordingly.

Based on the study in the thesis, the methodology of the performance based design for a multi-storey reinforced concrete frame structure against the distant blast loadings is summarized in Figure 7.1. After defining the expected performance level according to the requirements and objectives of the owners, users, and society for the frame structure under the given distant explosion conditions, the design is carried out for the reinforced concrete structural members using ESF.

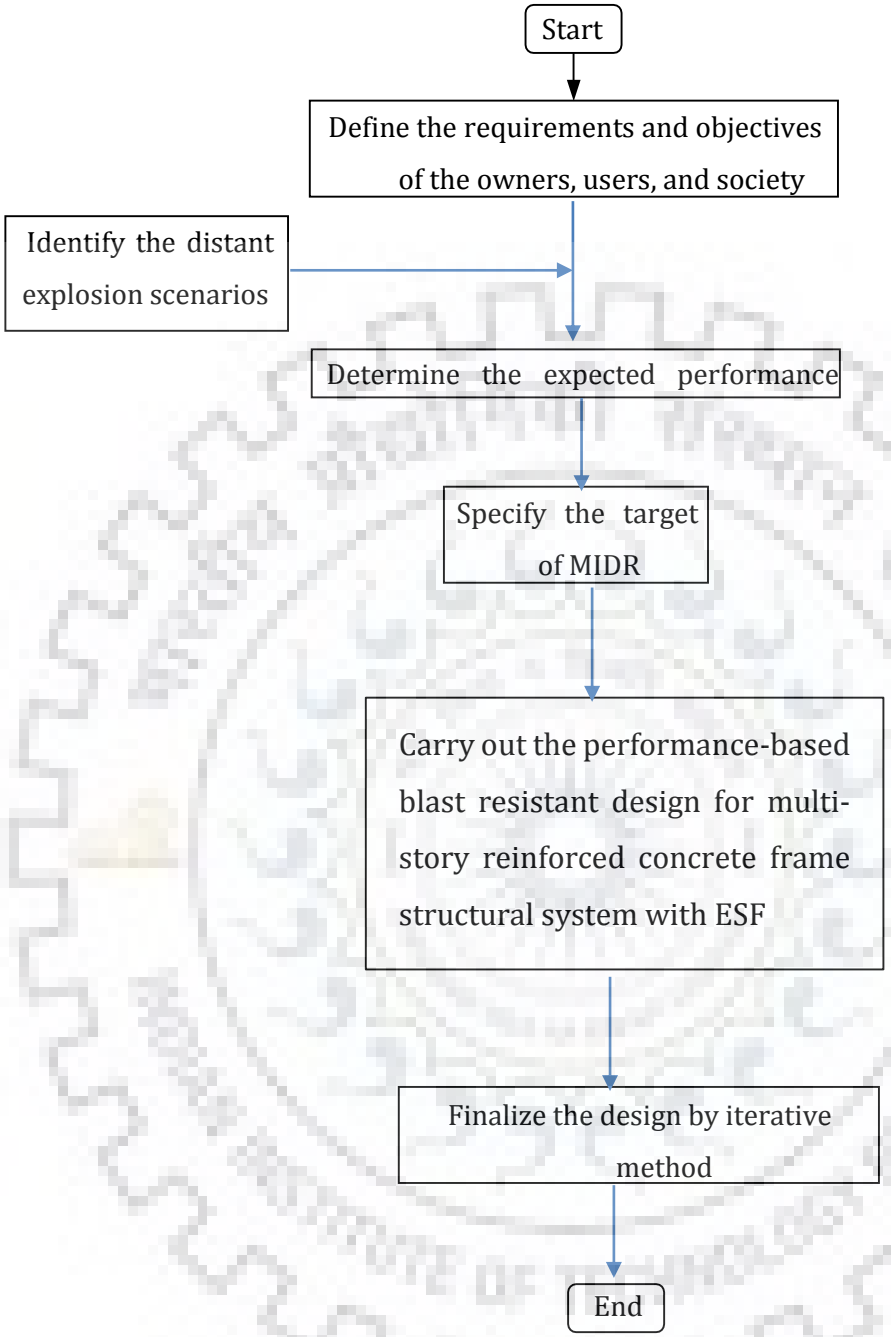

Fig. 7.1: Performance-based blast resistant design methodology of multi-storey reinforced concrete frame structures against distant explosions

7.3 RECOMMENDATIONS FOR FUTURE WORK

The following can be done in continuation of this thesis work.

1. The experimental verifications of the blast resistant design method with the ESF for the multi-storey reinforced concrete frame structures in controlling its MIDR responses should be conducted.
2. The explosion tests should be conducted for a frame structure with different types of exterior cladding panels in order to verify the numerical analytical results of the damage distributions.
3. The ESF based blast analysis of a SDOF system for maximum displacement was carried out for only elasto-plastic conditions. Further investigation needs to be carried out to determine the same for a strain hardening situation and a strain-softening situation.

REFERENCES

1. Biggs J. M. (1964), *Introduction to Structural Dynamic*, McGraw-Hill, New York.

2. Bounds WL. Design of blast resistant building in petrochemical facilities. ASCE Task Committee Report on Blast Resistant Design, 1997

3. Glasstone, S, & Dolan, P.J. (1977). *The effects of nuclear weapons*. US Department of Defense and the Energy Research and Development Administration, third edition.

4. Hai-Cheng Rong. Performance-based blast resistant design of reinforced concrete frame structures under distant explosions. PhD thesis, Nanyang Technological University, 2005.

5. Kang, B.S., Choi, W.S. & Park, G.F. (2001). Structural optimization under equivalent static loads transformed from dynamic loads based on displacement. *Computers and Structures*, 79, 145-154

6. Li, B., Rong, H.-C. & Pan, T.-C. (2007a). Drift-controlled design of reinforced concrete frame structures under distant blast conditions – part I: theoretical basis. *International Journal of Impact Engineering*, 34, 743-754.

7. Li, B., Rong, H.-C. & Pan, T.-C. (2007 b). Drift-controlled design of reinforced concrete frame structures under distant blast conditions – part II: implementation and evaluation. *International Journal of Impact Engineering*, 34, 755-770.

8. IS 4991 1968: Criteria for Blast Resistant Design of Structures for Explosions above Ground.

9. J H A Ruwan Jayasooriya, "Vulnerability and damage analysis of reinforced concrete framed buildings subjected to near field blast events". November 2010

10. Karlos V. and Solomos G. (2013), *Calculation of Blast Loads for Application to Structural Components*, European Laboratory for Structural Assessment, EU.

11. Koccaz Z. and Sutcu F. et. al. (2008), *Architectural and Structural Design for Blast Resistant Buildings*, Istanbul.

12. May G. C. and Smith P. D. (1995), *Blast Effect on Building: Design of Buildings to Optimize Resistance to Blast Loading*, Thomas Telford.

13. Mo, Y.L. (2004). Performance simulation of nuclear containments for security. *Journal of Performance of Constructed Facilities, ASCE*, 18 (2), 107-115.

14. NFEC (1986), *Blast Resistant Structures*, Naval Facilities Engineering Command, Design Manual 2.08, Alexandria, VA.

15. Paz, M. (2004). *Structural dynamics: theory and computation*. New Delhi, CBS Publishers & Distributors Pvt. Ltd.

16. TM5-1300, 1990, "Structures to Resist the Effects of Accidental Explosions", Technical Manual, US Departments of the Army, the Navy and the Air force

17. Yandzio E., Gough M. (1999). Protection of Buildings Against Explosions, SCI Publication, Berkshire, U.K.